

VILNIUS UNIVERSITY

MARIJA JANKUNEC

INVESTIGATION OF PROPERTIES OF LIPID LIQUID CRYSTALLINE DRUG CARRIERS  
AND THEIR INTERACTIONS WITH MODEL CELL MEMBRANES

Summary of doctoral dissertation  
Physical sciences, biochemistry (04 P)

Vilnius, 2013

The research was carried out at the Vilnius University Institute of Biochemistry during 2008–2012.

**Scientific supervisor**

dr. Justas Barauskas (Vilnius University, physical sciences, biochemistry – 04 P).

**The dissertation is defended at the Council of Biochemistry science direction of Vilnius University:**

**Chairman**

prof. habil. dr. Valdemaras Razumas (Vilnius University, physical sciences, biochemistry – 04 P).

**Members:**

habil. dr. Gediminas Niaura (Center for Physical Sciences and Technology, physical sciences, chemistry – 03 P);

dr. Augustas Pivoriūnas (State Scientific Research Institute Center for Innovative Medicine, physical sciences, biochemistry – 04 P);

dr. Vytautas Smirnovas (Vilnius University, physical sciences, biochemistry – 04 P);

dr. Ramūnas Valiokas (Center for Physical Sciences and Technology, physical sciences, physics – 02 P).

**Opponents:**

prof. dr. Rimantas Daugelavičius (Vytautas Magnus University, physical sciences, biochemistry – 04P);

dr. Rolandas Meškys (Vilnius University, physical sciences, biochemistry – 04 P).

Dissertation defense will take place at the Vilnius University Institute of Biochemistry (hall No 522, at 13:00) on 6<sup>th</sup> of June, 2013.

Address: Mokslininkų 12, LT-08662 Vilnius, Lithuania.

Summary of the dissertation has been sent out on 6<sup>th</sup> of May, 2013.

The dissertation is available at the libraries of Vilnius University and Vilnius University Institute of Biochemistry.

VILNIAUS UNIVERSITETAS

MARIJA JANKUNEC

LIPIDŲ SKYSTAKRISTALIŲ VAISTŲ NEŠIKLIŲ SAVYBIŲ IR JŲ SĄVEIKŲ SU LĄSTELIŲ  
MEMBRANŲ MODELIAIS TYRIMAS

Daktaro disertacijos santrauka  
Fiziniai mokslai, biochemija (04 P)

Vilnius, 2013

Disertacija rengta 2008–2012 metais Vilniaus universiteto Biochemijos institute.

**Mokslinis vadovas**

dr. Justas Barauskas (Vilniaus universitetas, fiziniai mokslai, biochemija – 04 P).

**Disertacija ginama Vilniaus universiteto Biochemijos mokslo krypties taryboje:**

**Pirmininkas**

prof. habil. dr. Valdemaras Razumas (Vilniaus universitetas, fiziniai mokslai, biochemija – 04 P).

**Nariai:**

habil. dr. Gediminas Niaura (Fizinių ir technologijos mokslų centras, fiziniai mokslai, chemija – 03 P);

dr. Augustas Pivoriūnas (Valstybinio mokslinių tyrimų instituto Inovatyvios medicinos centras, fiziniai mokslai, biochemija – 04 P);

dr. Vytautas Smirnovas (Vilniaus universitetas, fiziniai mokslai, biochemija – 04 P);

dr. Ramūnas Valiokas (Fizinių ir technologijos mokslų centras, fiziniai mokslai, fizika – 02 P).

**Oponentai:**

prof. dr. Rimantas Daugelavičius (Vytauto Didžiojo universitetas, fiziniai mokslai, biochemija – 04P);

dr. Rolandas Meškys (Vilniaus universitetas, fiziniai mokslai, biochemija – 04 P).

Disertacija bus ginama viešai 2013 m. birželio 6 d. 13 val. Vilniaus universiteto Biochemijos instituto aktų salėje (522 kab.).

Adresas: Mokslininkų 12, LT-08662 Vilnius, Lietuva.

Disertacijos santrauka išsiųsta 2013 m. gegužės 6 d.

Disertaciją galima peržiūrėti Vilniaus universiteto ir Vilniaus universiteto Biochemijos instituto bibliotekose.

## INTRODUCTION

In recent years a rising life expectancy, quick human pace of life are factors to look for to ensure a better quality of life. The smaller doses, more efficient in their operation, the decrease of side effects are features of drug delivery systems (DDS) which reduce patient discomfort or pain and, thus, improve the quality of life indicator. The development of lipid drug carriers is a minor technology of DDS. Lipids in an aqueous medium can self-assemble into the functional reversed phases. For decades, these non-lamellar liquid crystalline (LC) phases, which are stable in an aqueous environment, have been known to exist [1]. In response to the ambient properties they are able to release the bioactive substances. Lipid LC phases are characterized with properties as biodegradable, encapsulation of sensitive material and controlled release. It is known, that viscous reversed LC phases in excess water, for example, hexagonal ( $H_2$ ) and bicontinuous cubic ( $V_2$ ) [2] can be as sustainable drug release LC monolith. An encapsulated material can easily influence the inner nanostructure of one component drug carrier. So, two component systems should be far superior and more robust for environmental changes. One of these systems based on unsaturated components such (e.g. dioleoyl) phosphatidylcholine (PC) and glycerol dioleate (GDO). PC itself in water forms liquid-crystalline lamellar phase ( $L_\alpha$ ) [3] and GDO reversed micellar phase ( $L_2$ ) [4]. It is likely that these lipid-based mixtures will form a variety of non-lamellar phases.

In this thesis are described the phase behavior of lipid SPC/GDO liquid crystalline phases (LC monolith) and their dispersed nanoparticles (LCNPs). First of all, LC monolith pre-formulations are ideal for subcutaneous injection, so it is important to find out which phase transitions passes formed LC monolith. So, for this reason were simulated the limited and full hydration conditions. In the development of drug delivery systems crucial factor is not only hydration, temperature or incorporated drug influence on structural changes. The link between LC structure and the function of drug release is presented.

Recently, was introduced a mixture of lipids SPC, GDO and Polysorbate 80 for parenteral drug delivery [5], specially designed for preparation of stable LCNPs [6]. Only few studies had described the link between physical and chemical properties of non-lamellar lipid nanoparticles and their interactions with model phospholipid membranes [7, 8]. Hence in this thesis were studied the influence of surface chemistry, solution properties and size of nanoparticles on LCNPs behavior at the interface. In this case, the stability of the nanoparticles is important during the storage, the transport and the target adsorption. The interactions with different model surfaces were designed. These results will decide on further use of the studied lipid mixtures as release systems of bioactive materials.

**The aim of this work** is to study structural properties of lipid liquid crystalline drug carriers based on soya phosphatidylcholine (SPC), glycerol dioleate (GDO) and

water and their interactions with different surfaces. So, **the main objectives of the work** were as follows:

1. To investigate in detail the phase behavior of lipid SPC/GDO mixtures in the aqueous solutions.
2. To determine the influence of temperature on phase transitions of lipid SPC/GDO liquid crystals.
3. To evaluate the influence of nanostructure of lipid SPC/GDO liquid crystalline phases on sustained release of fluorescein.
4. To define the character of interactions of nanoparticles of lipid SPC/GDO liquid crystalline phases on hydrophobic, hydrophilic and cationic silica surfaces.
5. To estimate the efficiency of the fusion of nanoparticles of dispersed lipid SPC/GDO liquid crystalline phases with phospholipid liposomes and their hemolytic effect and to compare with nanoparticles formed by dispersed mono- and diglycerides based mixtures.
6. To evaluate the influence of the glycerol monooleate's concentration on the fusion efficiency of dispersed lipid SPC/GDO based nanoparticles with phospholipid liposomes and hemolysis.

### **The novelty and significance of the work**

The phase diagram of ternary soya phosphatidylcholine, diacylglycerol (mostly glycerol dioleate) and heavy water system was first described by Orädd [9]. However, this phase behavior of lipid SPC/GDO mixtures is a controversial and an incorrect with unresolved ranges of two and three phases. Due to the formation of self-assembled structures such mixtures are attractive and promising as drug delivery systems. In this thesis for this purpose in detail was described the new phase behavior of lipid SPC/GDO mixtures in more relevant physiological conditions. And structural properties of the drug carrier were related with an active material's release profile. Thus, it will be easier to program and construct the drug carrier of desirable properties.

Lipid liquid crystalline nanoparticles can be used for an encapsulation of lipophilic and water-soluble drugs and an intravenously administration. It is important that such carriers will be lacked of hemolytic activity, i.e. to be safe and tolerable. This work reveals that liquid crystalline nanoparticles of dispersed lipid SPC/GDO mixtures have low hemolytic activity, and more likely than others investigated LCNPs fit for an intravenous drug delivery. For the first time were investigated the adsorption properties of these nanoparticles on different modified silica surfaces.

### **The defense statements of the work**

- By changing the ratio of soya phosphatidylcholine and glycerol dioleate it is possible to control and vary the sustained release of the encapsulated material.
- By changing the surface properties it is possible to control the adsorption of dispersed lipid SPC/GDO-based nanoparticles.

- *In vitro* studies of nanoparticles of dispersed lipid liquid crystalline phases enable to prognosticate their behavior *in vivo*.

### **Dissertation contents and approbation**

Dissertation (in Lithuanian) contains 138 pages, 49 figures, 10 tables and 181 entries in the reference list. Four publications have been published in the international scientific journals on the theme of dissertation. The research results have been presented at 2 national and 6 international scientific conferences.

### **List of papers**

*Paper I:* Tiberg F., Johnsson M., **Jankunec M.**, Barauskas J. Phase behavior, functions and medical applications of soy phosphatidyl choline and diglyceride lipid compositions. *Chemistry Letters* 41 (2012): 1090–1092.

*Paper II:* Chang D. P., **Jankunec M.**, Barauskas J., Tiberg T., Nylander T. Adsorption of lipid liquid crystalline nanoparticles on cationic, hydrophilic, and hydrophobic surfaces. *ACS Applied Materials & Interfaces* 4 (2012): 2643–2651.

*Paper III:* Chang D. P., **Jankunec M.**, Barauskas J., Tiberg T., Nylander T. Adsorption of lipid liquid crystalline nanoparticles: effects of particle composition, internal structure, and phase behavior. *Langmuir* 28 (2012): 10688–10696.

*Paper IV:* Barauskas J., Cervin C., **Jankunec M.**, Spandyreva M., Ribokaite K., Tiberg F., Johnsson M. Interactions of lipid-based liquid crystalline nanoparticles with model and cell membranes. *International Journal of Pharmaceutics* 391 (2010): 284–291.

### **Contribution report to the papers**

*Paper I:* I did most of experimental work and data evaluation in the study and, also, I participated in the interpretation of data.

*Paper II and Paper III:* I was responsible for samples preparation for SAXD measurements, experimental work and for data analysis.

*Paper IV:* I was responsible for FRET (fluorescence) measurements: participated in the planning of the study and the interpretation of data, supervised the main experimental work.

### **Conference materials/abstracts**

1. **Jankunec M.**, Harwigsson I., Thuresson K., Johnsson M., Barauskas J., Kocherbitov V. The phase behavior of dioleoylphosphatidylcholine in water. 26<sup>th</sup> European Colloid and Interface Society (ECIS2012) meeting. 2012 September (Malmö, Sweden). Poster presentation.

2. **Jankunec M.**, Persson L., Tiberg F., Johnsson M., Barauskas J. Hydration behavior, functions and medical applications of soy phosphatidylcholine and diglyceride lipid compositions. 26<sup>th</sup> European Colloid and Interface Society (ECIS2012) meeting. 2012 September (Malmö, Sweden). Poster presentation.

3. **Jankunec M.**, Johnsson M., Barauskas J., Kocherbitov V. The aqueous phase behavior of dioleoylphosphatidylcholine. Biofilms 7th annual workshop. Biomaterials:

From Fundamentals to Market Application. 2011 October (Malmö, Sweden). Poster presentation.

4. **Jankunec M.**, Johnsson M., Tiberg F., Barauskas J. The phase behavior of aqueous soy phosphatidylcholine/glycerol dioleate mixtures. 25<sup>th</sup> European Colloid and Interface Society (ECIS2011) meeting. 2011 September (Berlin, Germany). Poster presentation.

5. **Jankunec M.** Lipidų matricių struktūriniai tyrimai. Projekto "Studentų mokslinės veiklos skatinimas" dalies "Doktorantų stažuotės užsienio mokslo centruose" dalyvių konferencija. 2011 March (Vilnius, Lithuania). Oral presentation.

6. **Jankunec M.**, Barauskas J., Tiberg F., Johnsson M. "SAXS study of the phase behavior of aqueous soy phosphatidyl choline/ glycerol dioleate mixtures", 23rd Annual MaxLab User meeting. 2010 November (Lund, Sweden). Poster presentation.

7. **Jankunec M.**, Cervin C., Špandyreva M., Ribokaitė K., Tiberg F., Johnsson M., Barauskas J. Interactions of lipid-based liquid crystalline nanoparticles with model and cell membranes. Biofilms 6th annual workshop. Biomaterials: From Fundamentals to Market Application. 2010 October (Malmö, Sweden). Poster presentation.

8. **Jankunec M.**, Cervin C., Špandyreva M., Ribokaitė K., Tiberg F., Johnsson M., Barauskas J. Interactions of lipid-based liquid crystalline nanoparticles with model membranes. 15-oji Tarptautinė studentų ir jaunųjų mokslininkų konferencija "Chemija ir cheminė technologija 2010". 2010 May (Vilnius, Lithuania). Oral presentation.

## ABBREVIATIONS

**d** - repeat distance; **DHPE** - 1,2-dihexadecanoyl-sn-glycero-3-phosphoethanolamine, triethylammonium salt, rhodamine B; **F127** - Pluronic, poly(ethylene oxide)-poly(propylene oxide)-poly(ethylene oxide) tri-block copolymer; **Fd3m** - space group of face-centered cubic phase; **Fluo** - fluorescein disodium salt; **FRET** - Förster resonance energy transfer; **GDO** - glycerol dioleate; **GMO** - glycerol monooleate; **H<sub>2</sub>** - reversed hexagonal phase; **hcp** - hexagonal close packing; **I<sub>2</sub>** - reversed cubic phase; **L<sub>2</sub>** - reversed micellar phase; **LC** - liquid crystal, liquid crystalline; **LCNPs** - lipid liquid crystalline nanoparticles; **L<sub>α</sub>** - liquid crystalline lamellar phase; **NBD-PE** - N-(7-nitrobenz-2-oxa-1,3-diazol-4-yl)-1,2-dihexadecanoyl-sn-glycero-3-phosphoethanolamine, triethylammonium salt; **P6<sub>3</sub>/mmc** - space group of 3-D hexagonal inverse micellar lyotropic phase; **P80** - Polysorbate 80, polyoxyethylene (20) sorbitan monooleate; **PEO** - poly(ethylene oxide); **PdI** - polydispersity index; **SAXD** - small angle X-ray diffraction; **SPC** - soya phosphatidylcholine.



## MATERIALS and METHODS

### Chemicals

**Lipids:** soya phosphatidylcholine (S100 from Lipoid GmbH, Germany) with the major components phosphatidylcholine (> 94 %), triglycerides (< 1 %), lysophosphatidylcholine (< 1.0 %) and free fatty acid (<0.05 %). Glycerol dioleate containing diglycerides (96 %), monoglycerides (0.2 %) and triglycerides (3.8 %); glycerol monooleate containing monoglycerides (95 %) and diglycerides (4.1 %); diglycerol monooleate (DGMO) containing diglycerol monoester (87 %), glycerol monoester (2 %) and free glycerol and polyesters (5.2 %) (Danisco, Denmark). 1,2-Dioleoyl-*sn*-glycerol-3-phosphocholine (DOPC, > 99 %) was obtained from Avanti Polar Lipids (USA). **Surfactants:** polyoxyethylene (20) sorbitan monooleate (Apoteksbolaget AB, Sweden); and poly(ethylene oxide) (PEO)–poly(propylene oxide) (PPO)–poly(ethylene oxide) tri-block co-polymer (BASF Svenska AB, Sweden) with the trade name Pluronic® F127 and approx. formula of PEO<sub>98</sub>PPO<sub>67</sub>PEO<sub>98</sub> (average molecular weight of 12.600 g/mol). Triton X-100 (Loba Chemie PVT. LTD., India). **Fluorophores:** N-(7-nitrobenz-2-oxa-1,3-diazol-4-yl)-1,2-dihexadecanoyl-*sn*-glycerol-3-phosphoethanolamine, triethylammonium salt and 1,2-dihexadecanoyl-*sn*-glycerol-3-phosphoethanolamine, triethylammonium salt (Lissamine™, rhodamine B) were obtained from Invitrogen (Invitrogen, USA). Fluorescein disodium salt (Fluka, Switzerland). All other solvents and reagents were of analytical grade and were used as received. Milli-Q purified water (18.2 MΩcm) was used for all experiments. **Figure 1** presents structures of lipids and polymer used in this work.

### Bulk lipid liquid crystalline sample preparation

Samples were prepared by mixing appropriate amounts of lipids (total lipid amount of ca. 0.2–0.4 g) in 10 wt. % ethanol to facilitate mixing. The samples were placed on a roller mixer for over an hour until mixed completely. Pre-formulations were kept in a freezer at –18 °C until further use. In some cases ethanol from the samples was removed by a rotating rotor with a water pump (IKA, Germany). Non-aqueous lipid mixtures prepared in such way contained less than 1 wt. % of ethanol, which was controlled by weighing samples before and after drying procedure. Afterwards, the samples were respectively hydrated.

### Lipid liquid crystalline phases

Liquid crystalline (LC) phases were prepared from their pre-formulation by using different protocols: (i). at full hydration conditions LC samples in excess saline or water were prepared by mixing pre-formulations with saline at a ratio 10/90 (wt. %/wt. %), intensively vortexed for few minutes and left to equilibrate on a roller mixer for at least 3 weeks before experiments. Excess saline LC samples were prepared in such a way that final concentration of ethanol was 1 wt. %. (ii) The LC samples without ethanol at limited saline concentration conditions. In order to hydrate non-aqueous samples, the required amounts of water (5–50 wt. % with respect to the total sample mass) were added; samples were immediately sealed and left to

equilibrate at room temperature (RT) for at least 3 weeks before experiments. To obtain phase homogeneity in the *protocols (i) and (ii)*, during equilibration time hydrated samples were centrifuged with the sample containers up and down several times (2–3 min, 1500xg). *(iii)* Water penetration experiments were performed using HR6-124 (80 mm with inner diameter of 1.6–1.8 mm) one side sealed glass capillaries (Hampton Research, USA). Bottom of capillary (approx. 30 mm) was filled with non-aqueous SPC/GDO formulation and approx. 30 mm of saline solution was added on top of lipid formulation. The top was flame sealed and lipid formulations were left to swell for 5–21 days keeping capillaries in vertical position.

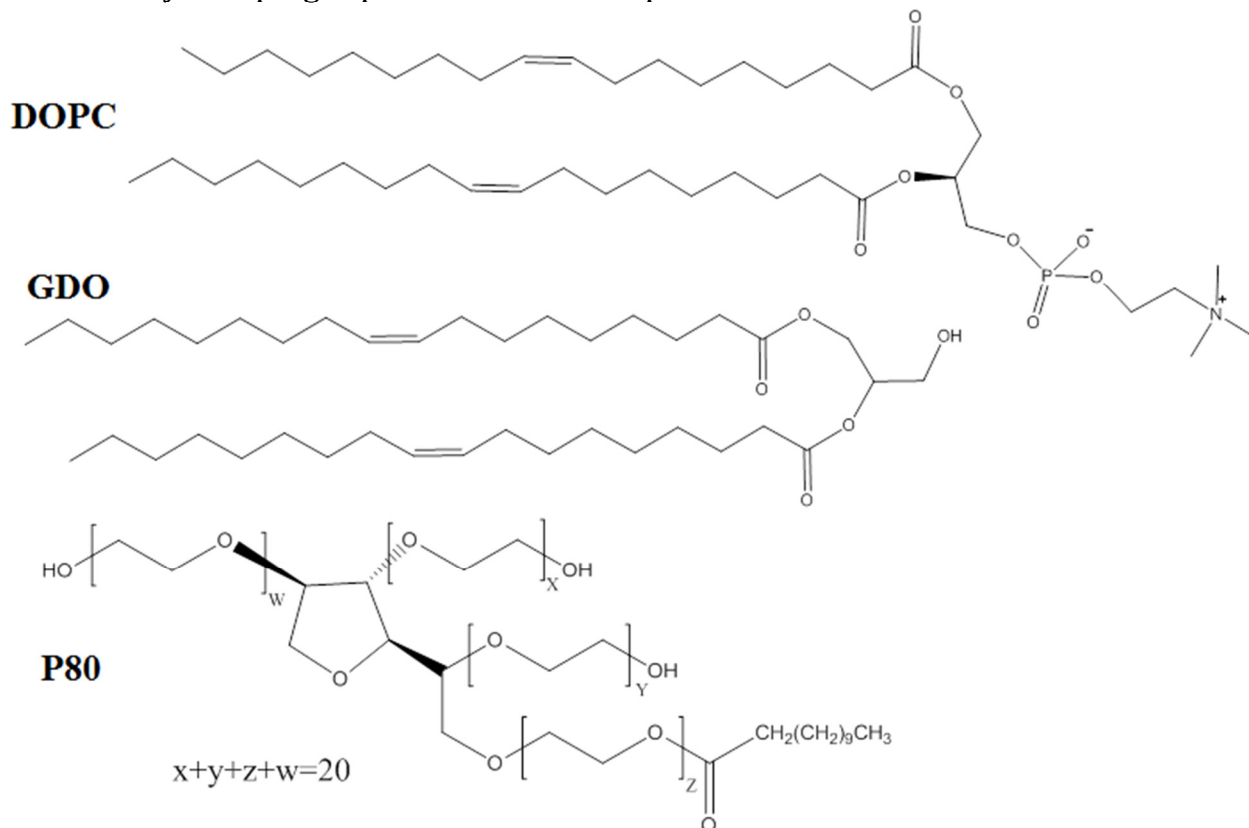


**Figure 1.** Structures of mainly used in this work lipids and polymer

### Preparation of lipid-based liquid crystalline nanoparticles

Nanoparticles of lipid liquid crystalline phases were prepared from LC pre-formulations dispersed in aqueous solution with added stabilizer. Aqueous LCNPs dispersions (5 wt. % of lipid) were prepared by adding appropriate amount of pre-formulation to pure water (or to 5 wt. % glucose solution for use in the hemolysis assay). Samples were then immediately sealed, hand-shaken and left to vortex for 48–72 h on a shaking table (180–400 rpm, 30 °C). Heat treatment of the mechanically shaken dispersions was performed using a bench-type autoclave (125 °C; 1.4 bar; during 20 min). After the heat treatment, the samples were allowed to cool to RT. Afterwards, 5 wt. % dispersions of nanoparticles were diluted in saline. **Preparation of LCNPs with entrapped fluorescent lipids:** NBD-PE (donor) and rhodamine DHPE

(acceptor). 0.4 mg NBD-PE or 0.5 mg rhodamine DHPE were diluted in 1.250 mL mixture of chloroform/ethanol (ratio 1:4 v/v); final concentration of solutions 0.335 mM and 0.3 mM, respectively. 8  $\mu$ M the solution of fluorescent NBD-PE/DHPE lipids (1:1) was prepared from 0.24 mL NBD-PE and 0.27 mL DHPE of basic solutions mixed in 19.49 mL ethanol. For labeling of particles dispersions, an amount (80–150  $\mu$ L) of 8  $\mu$ M of fluorescent lipid solution were added to 6 mL 0.003 % LCNPs dispersions in such a way that final concentration of fluorophore was 1 mol%. Before each measurement dispersions were left to vortex for 48 h.

### **Preparation dispersion of coarse multilamellar or unilamellar liposomes**

Coarse dispersions of multilamellar liposomes were prepared by adding 2.25 g of SPC to 47.75 mL 0.9 wt. % NaCl solution. The samples were immediately sealed, hand-shaken and left to vortex for 48–72 h on a shaking table ( $\sim$  29  $^{\circ}$ C, 180 rpm).

Unilamellar liposomes comprising SPC or SPC/DOPE–PEG (2000) (PEG-lipid) were prepared by dissolving the lipid or lipid mixture in chloroform followed by evaporation of the solvent under vacuum to form dry lipid films. Hydration of the lipids was performed in saline by repeated freeze–thawing (freezing in liquid nitrogen and thawing in water bath at 50  $^{\circ}$ C) with intermittent vortex mixing. The dispersions were thereafter extruded through 2 stacked polycarbonate filters of pore size 400 nm 15 times using a LIPEX extruder (Avanti Lipids Inc., Canada) to form unilamellar liposomes.

### **Hemolysis (the interaction with erythrocytes)**

Fresh whole blood (heparinized) from rat was mixed with lipid dispersions, prepared as described above (5 wt. % total lipid dispersed in an aqueous medium containing 5 wt. % glucose), or controls in a ratio of 1:1 (vol./vol.) (total volume of 1 mL). 5 wt. % glucose in water for injection (WFI) and 2 wt. % Triton X-100 (surfactant) in WFI were used as negative and positive controls, respectively. Samples were incubated at 37  $^{\circ}$ C with gentle rotation at 200 rpm on a shaking table during 1 h, after which they were centrifuged at 2000 $\times$ g during 10 min. Supernatants were treated with aqueous 10 wt. % Triton X-100 solution in a ratio of 1:4 (vol./vol.) (total volume of 200  $\mu$ L) to prevent false positive results originating from the turbidity of the lipid dispersions. Absorbance of the Triton X-100 treated supernatant was determined spectrophotometrically in a 96-well microtiterplate at 540 nm. Hemolysis was reported as % of positive control (100 % hemolysis) according to:

$$\frac{Abs_{sample} - Abs_{negative}}{Abs_{positive} - Abs_{negative}} \times 100 \quad (1)$$

### ***In vitro* release experiments**

Non-aqueous lipid pre-formulations comprising fluorescein (Fluo) were prepared in 6 mL vials by weighing 10 mg of Fluo and 1.99 g of SPC/GDO mixture containing 10 wt. % of ethanol. After brief vortex mixing the vials were placed on a roller mixer until homogeneous solutions were obtained. The *in vitro* release experiments were performed in 8 mL vials by injecting 100 mg of the pre-formulation

into 5 mL phosphate buffered saline (PBS, pH 7.4). Sterile BD Plastipak (KA, USA) 1 mL syringes and 18 G needles were used. Triplicate samples for each composition were used. The vials were sealed and placed on a shaking table at 150 rpm at 37 °C. At the sampling points (after 2, 4 and 7 days) 0.1 mL of the aqueous phase was removed and diluted 15 times with PBS. The concentration of Fluo was determined spectrophotometrically by using Lambda 40 spectrophotometer (Perkin Elmer) equipped with EL808IU micro plate reader (BioTek) and 96-well plate. 0.3 mL of sample was added to each well and the absorbance was measured at 490 nm. The concentration and released amount of Fluo (in %) was calculated using the calibration curve obtained for each plate. The calibration curves were obtained by measuring absorbance of Fluo solutions in PBS in a concentration range of 0.00016–0.0134 mg/mL. Calibration curves for all plates resulted in straight lines with  $r^2 = 0.995$ . Pre-formulations with 0.5 wt. % Fluo were added to water in ratio 1:10, thus ethanol concentration is less than 1 wt. %. Formulations were pictured in time. Also to compare, various formulations were prepared in saline (37 °C).

### **Small-angle X-ray diffraction**

Synchrotron SAXD measurements were performed at the I711 beamline at MAX-lab (Lund University, Sweden), using a Marresearch 165 mm CCD detector mounted on a Marresearch Desktop Beamline baseplate [10, 11]. Bulk lipid/water (or saline) liquid crystalline samples were mounted between kapton windows in a steel sample holder at the sample-to-detector distance of 1250–1683 mm. For water penetration experiments diffractograms were directly recorded from horizontally placed sealed glass capillaries. Sample movement along x-axis of the capillary was controlled within 0.1 mm. Diffractograms were recorded at 25 °C (in some cases in the range 5–75 °C, an equilibration time of 10 min at given temperature) under high vacuum with a wavelength of 0.1066–0.1201 nm and the beam size of  $0.25 \times 0.25$  mm (full width at the half-maximum) at the sample. Typical exposure time was 3–5 min. The resulting CCD images were integrated and analyzed using the Fit2D software [12]. The calibrated wavelengths and detector positions were used.

### **Fluorescence measurements**

All fluorescence experiments were performed using LS 55 Fluorescence Spectrometer (PerkinElmer, USA). FRET (Förster resonance energy transfer) experiments were performed by entrapping fluorescent probes (0.5 mol% NBD-PE and 0.5 mol% DHPE) within the dispersed LCNPs, allowing the labeled LCNPs to mix with SPC liposomes, and following fluorescence emission decays with time for 30 min at 580 nm [13]. Briefly, 2 mL of prepared LCNPs (0.003 wt. % with respect to lipid) labeled with 1 mol% of fluorescent phospholipids (0.5 mol% of DHPE and 0.5 mol% of NBD-PE) were added to 1 cm path length quartz cuvettes and mixed with 13  $\mu$ L 4.5 wt. % SPC multilamellar liposomes. The obtained fluorescence decay curves were background corrected (intensity data from mixing SPC liposomes with LCNP dispersions without fluorescent probes were subtracted), and normalized (initial

intensity was set to 100 %). To mimic *in vivo* conditions as closely as possible, all FRET mixing experiments were deliberately performed at a LCNP/SPC liposomes weight ratio of 1/10 (wt. %/wt. %).

### Ellipsometry

The oxidized substrates used throughout this work were silica surfaces prepared from polished silicon wafers (p-type, boron-doped, resistivity of 1–20  $\Omega$  cm) (Linköping University (Sweden) and SWI (Taiwan)). The cationic silica surfaces were prepared by liquid-phase silanization, the hydrophobic silica surfaces by gas-phase silanization and the chitosan-coated surfaces by adsorbing chitosan in water to the plasma cleaned silica surface. The adsorption measurements were monitored *in situ* by null-ellipsometry as described previously [14, 15]. The sample cell was thermostated to 25 °C and agitated with a magnetic stirrer. Measurements were done with an angle of incidence around 67.85°. Before each experiment, the silica surface properties were determined using a three-layer substrate model, assuming bulk isotropic silicon with a thin layer of oxide in an ambient media. The absorbed amount,  $\Gamma$ , then can be calculated using de Feijter's approximation [16]:

$$\Gamma = \frac{(n-n_0)d}{dn/dc}, \quad (2)$$

where  $n_0$  is the refractive index of the solvent and  $dn/dc$  is the refractive index increment of the adsorbed materials as a function of its bulk concentration. After surface characterization, measurements were conducted by injecting 10  $\mu$ L of the concentrated LCNPs dispersion (5 wt. %, 50 mg/mL) into the cuvette to a final concentration of 0.1 mg/mL.

## RESULTS and DISCUSSION

Non-lamellar LC phases based on soya phosphatidylcholine and glycerol dioleate mixtures due to their properties may be accommodate to sustained and slow drug release [6, 17], either in the forms of *in vivo* forming liquid crystalline structures, or dispersed into LC nanoparticles. Pre-formulations of liquid crystalline phases are suitable for drug release subcutaneously and their dispersed systems (nanoparticles) intravenously. Thus, the studies of these systems are independent. First of all, we will discuss about the phase behavior of lipid SPC/GDO mixtures. In the second part, properties of dispersed lipid mixtures are described and their interactions with model cell membranes and modified silica surfaces.

### I. The phase behavior of soya phosphatidylcholine and glycerol dioleate

A schematic illustration of the evolution of the injected subcutaneously lipid system is shown in **Figure 2** in order to better understand the observed *in vitro* release behavior and the processes involved. Several processes occur simultaneously all of them influencing the release properties of the system: formation of LC shell and

lipid self-assembly, water penetration and solvent release, increase of the LC shell thickness. All these processes and also the kinetics of the LC shell formation and the nanostructure of the LC aggregates will influence the release properties of the system. It is therefore the determination of equilibrium and non-equilibrium phase behavior of the lipid SPC/GDO mixtures is of an utmost importance.

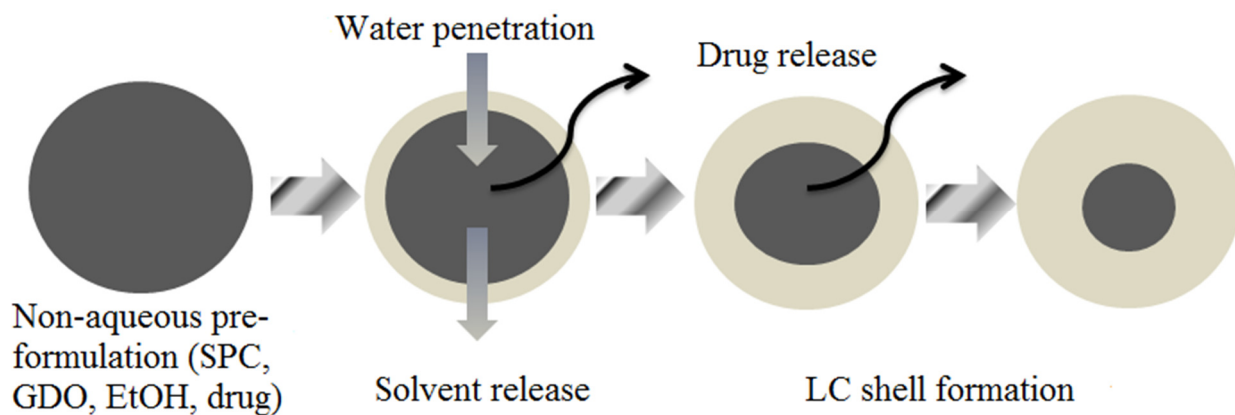


**Figure 2.** A schematic illustration of the LC monolith formation

The processes involved after the contact of the non-aqueous lipid pre-formulation with aqueous media: absorption and penetration of water and lipid self-assembly, LC shell formation and drug release. All processes occur simultaneously. *Abbr.:* EtOH – ethanol.

### The influence of the solvent

Ethanol (EtOH) is added to pre-formulations of lipid SPC/GDO LC phases to homogenize mixtures. It is desirable that an injected semi-liquid drug carrier exhibit low viscosity properties. To estimate EtOH concentration limit when transition from reversed micelles ( $L_2$ ) into non-lamellar LC phases is performed, SAXD data collected from the lipid SPC/GDO mixtures with different concentrations of ethanol in range 7–20 wt. % in saline 0–90 wt. % ratio. When the concentration of EtOH is 7 wt. % (of the total lipid mass), 5 wt. % saline is sufficient to form LC phase. This phase occurs almost immediately after contact with an aqueous medium. Next, the phase behavior of two mixtures is similar to each other when EtOH content is 10 and 12 wt. %, respectively. However, only at a full hydration conditions (90 wt. % saline) in 10 wt. % EtOH well-defined reverse hexagonal ( $H_2$ ) phase was formed. Meanwhile, for formation of non-lamellar LC phases when EtOH content is 16 and 20 wt. % the systems require 30 and 40 wt. % of saline solution, respectively. So, all studied LC phase pre-formulations were prepared with 10 wt. % ethanol, which was evaporated if samples at the limited hydration were prepared.

### The phase behavior in excess water

We have studied in detail the equilibrium phase behavior and phase structures for the two-component lipid SPC and GDO mixtures as a function of lipid composition in excess water. **Figure 3** presents the measured SAXD profiles of fully hydrated (90 wt. %) mixtures of SPC/GDO between lipid ratios of 70/30 and 20/80 by weight at every 2.5 wt. %. As seen from SAXD data the phase behavior of SPC/GDO is indeed rich and complex. Soya phosphatidylcholine – is a mixture of lipids extracted from soya

beans, mainly contains phosphatidylcholine with C<sub>16</sub> – C<sub>18</sub> long chains, with one or two double bonds. And it has some non-PC impurities.

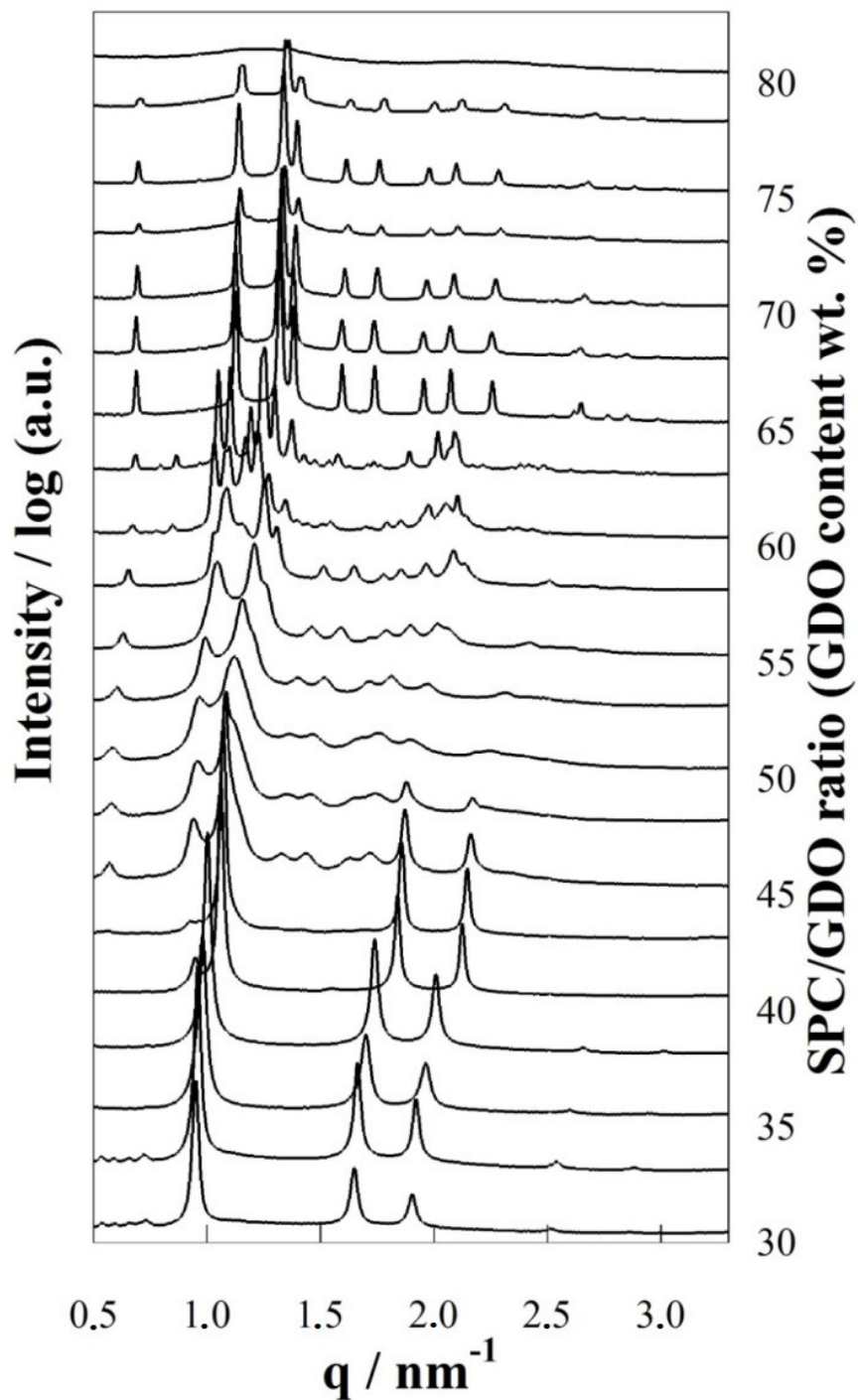


**Figure 3.** SAXD profiles of fully hydrated mixtures of SPC/GDO

SAXD profiles as a function of lipid composition between SPC/GDO weight ratios of 70/30 and 20/80, at 25 °C.

At low GDO content and up to SPC/GDO weight ratio of 62.5/37.5 a  $2D-H_2$  phase is formed which is characterized by five distinctive reflections at relative positions in

ratios of 1: $\sqrt{3}$ :2: $\sqrt{7}$ :3. The calculated lattice parameter ( $a$ ) of 2D- $H_2$  phase decreases from 7.66 to 7.25 nm between SPC/GDO ratio of 70/30 and 62.5/37.5. With increasing GDO content a cubic phase starts to emerge, which one-phase region exists between SPC/GDO ratios of 50/50 and 45/55. This is clearly shown by the location of the relative positions in ratios of the first 9 Bragg peaks, being  $\sqrt{3}:\sqrt{8}:\sqrt{11}:\sqrt{12}:\sqrt{16}:\sqrt{19}:\sqrt{24}:\sqrt{27}:\sqrt{32}$ , which can be indexed as the reflections of a face-centered  $I_2$  phase of  $Fd\bar{3}m$  space group (Figure 4 a). With increasing GDO content the obtained  $a$  value for this phase varies from 18.7 down to about 17.3 nm, related to the increasing negative curvature and/or decreasing swelling ability of the cubic phase.

At even higher GDO concentration, an extremely narrow region of another LC phase is located between SPC/GDO weight ratios of approximately 42/58 and almost 40/60 (Figure 4 b). 20 Bragg peaks were identified which positions and indexing are summarized in **Table 1**. Indexing of SAXD data of this phase was achieved assuming 3D hexagonal close packing ( $hcp$ ) structure. The analysis clearly shows that the structure of this phase is consistent with the  $hcp$  lattice of identical spherical reversed micelles having  $P6_3/mmc$  symmetry. The following relation was used where the  $d_{hkl}$  is related to the two lattice parameters,  $a$  and  $c$ , and where  $R=c/a$ :

$$\frac{1}{d_{hkl}^2} = \frac{1}{a_{hkl}^2} \left( \frac{4}{3} (h^2 + k^2 + hk) + \frac{l^2}{R^2} \right) \quad (3)$$

**Table 1.** Indexing of the 3D hexagonal phase with  $P6_3/mmc$  symmetry formed in fully hydrated SPC/GDO mixtures of 40/60 (wt. %/wt. %) composition using lattice parameters  $a=69.85$ ,  $c=113.5$

No.	$hkl$	Calculated $2\Theta$	Observed $2\Theta$	No.	$hkl$	Calculated $2\Theta$	Observed $2\Theta$
1	0 1 0	0.862	0.862	11	0 2 2	1.953	1.952
2	0 0 2	0.919	0.919	12	0 1 4	2.030	2.028
3	0 1 1	0.977	0.978	13	0 2 3	2.207	2,205
4	0 1 2	1.260	1.260	14	1 2 0	2.281	2,278
5	1 1 0	1.493	1.494	15	1 2 1	2.326	2.325
6	0 1 3	1.626	1.628	16	1 1 4	2.368	2.365
7	0 2 0	1.724	1.727	17	0 1 5	2.453	2.455
8	1 1 2	1.753	1.752	18	0 3 0	2.586	2.584
9	0 2 1	1.784	1.779	19	1 2 3	2.665	2.662
10	0 0 4	1.838	1.832	20	0 3 2	2.744	2.745

The calculated lattice parameters for this 3D hexagonal phase are  $a = 6.99$  and  $c = 11.35$  nm with a  $c/a$  ratio of 1.624 which is very close to the value for ideal  $hcp$  lattice of identical spheres,  $R_{ideal}=\sqrt{8/3}=1.633$ . In addition, the intensities of obtained



SAXD reflections are similar to those obtained for 3D hexagonal  $P6_3/mmc$  phase of DOPC/GDO/cholesterol [18] and surfactant [19] systems in water.

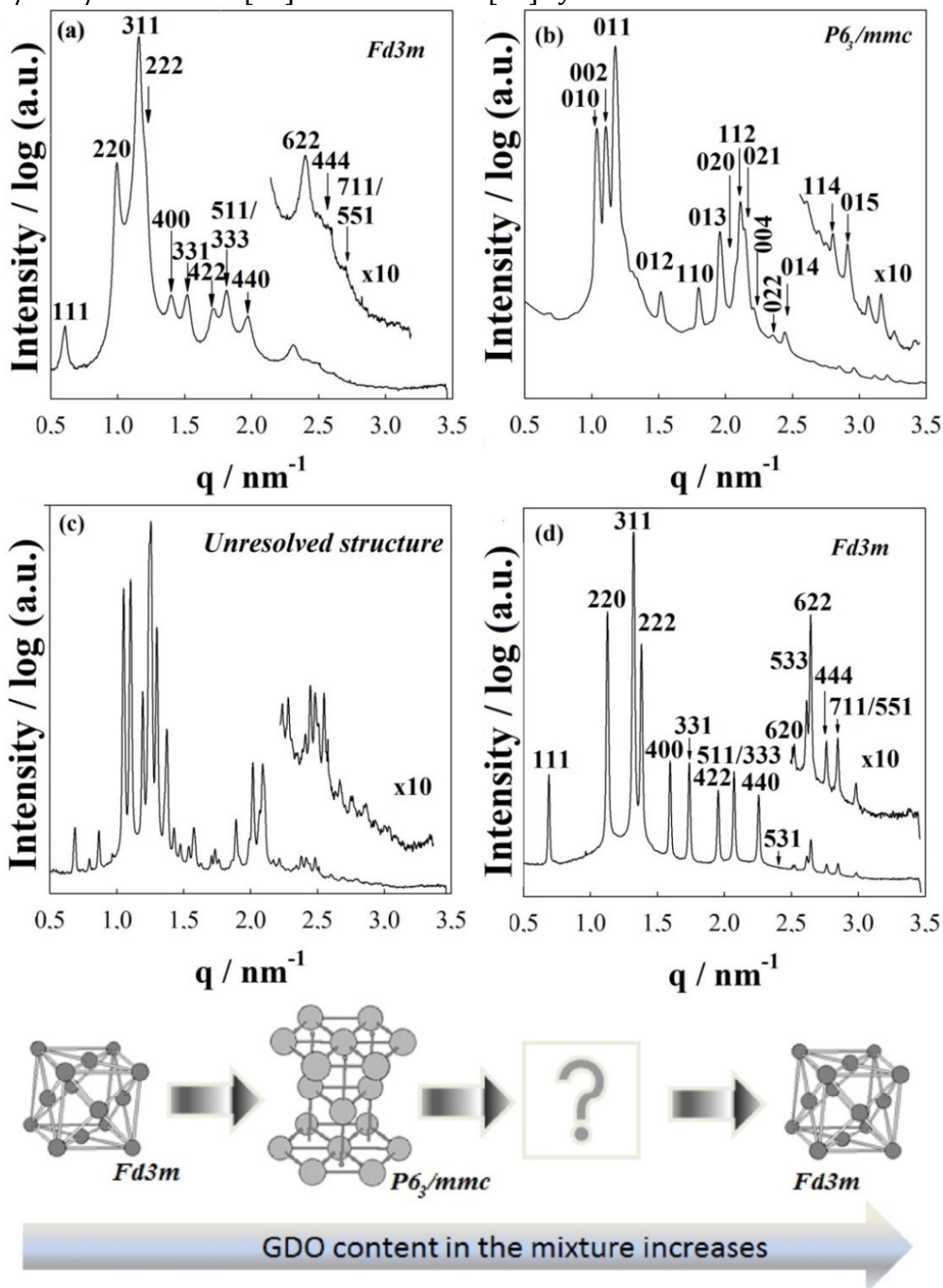


**Figure 4.** Representative SAXD profiles of the LC phases of fully hydrated mixtures of SPC/GDO SAXD profiles as a function of lipid composition at 25 °C. SPC/GDO weight ratios are: 47.5/52.5 (a), 40/60 (b), 37.5/62.5 (c), and 35/65 (d). LC structures in SAXD profiles are characterized with Miller indices.

Between SPC/GDO weight ratios of approximately 39/61 and 37/63 a very narrow region of yet another LC phase was identified (Figure 4 c). It shows at least 30 Bragg reflections which are not consistent with neither cubic nor 3D hexagonal lattices of neighboring phases and we were unable to resolve its structure. We can only speculate that since it is between  $P6_3/mmc$  and  $Fd3m$  phases its structure should be “intermediate” between hexagonally close packed identical micelles and the cubic  $Fd3m$  lattice consisting of two types of reversed micelles. Starting from SPC/GDO ratio of 35/65 the cubic  $Fd3m$  phase is found again which shows very nice SAXD pattern with at least 15 Bragg peaks (Figure 4 d). With increasing GDO content the calculated  $a$  value for this phase decreases from about 15.81 to 15.42 nm before transforming into reversed micellar phase ( $L_2$ ) at SPC/GDO weight ratio of 20/80.

In conclusion, at 25 °C with increasing GDO content fully hydrated SPC/GDO mixtures form the following LC phase sequence: lamellar ( $L_\alpha$ ) → reversed 2D hexagonal ( $H_2$ , up to 62.5/37.5) → reversed micellar cubic of  $Fd3m$  space group (50/50 – 45/55) → reversed 3D hexagonal of  $P6_3/mmc$  space group (42/58 – 40/60) → unresolved “intermediate” (39/61 – 37/63) →  $Fd3m$  (35/65 – 22.5/77.5) → reversed micellar solution ( $L_2$ , from 20/80). Note, that re-appearance of the  $Fd3m$  phase at different GDO content is not surprising and does not contradict the Gibbs phase rule. These two phases are indeed interconnected at limited hydration values and form a one-phase region. Our findings show that the two component diacyl lipid system is rich in phase behavior.

The intricate phase behavior of fully hydrated mixtures of SPC/GDO described here has not been observed before. Most of the studies were performed with mixtures of dioleoylphosphatidylcholine/GDO, show a less rich phase behavior [20, 21]. Here it should also be noted that contrary to our findings, previously determined phase behavior of fully hydrated SPC/GDO also show no formation of  $P6_3/mmc$  and “intermediate” unknown phase [9]. The reason for this difference is that the authors in that study used  $D_2O$  instead of  $H_2O$ .

### **The influence of temperature**

To closer mimic *in vivo* conditions here we have studied the lipid mixing phase behavior in physiologically relevant environment by using saline and appropriate temperatures. The phase behavior results of SPC/GDO mixture obtained in excess saline (90 wt. %) are similar to those in excess water. Both systems describes the same phase behavior at 25 °C, the only difference is that for saline-based mixtures the phase transition boundaries are somewhat shifted towards lower GDO content as compared with the water-based system. It is important, that the increased temperature to physiologically more relevant (37–42 °C) have an effect on the stability of  $P6_3/mmc$ , unresolved structure and  $Fd3m$  phase (Figure 5). Thus, the SPC/GDO/saline mixture at 42 °C has only 3 of the 5 different regions:  $2D-H_2$  phase transforms into a disordered, similar to the  $Fd3m$  structure at SPC/GDO weight ratio of 50/50, in turn, reversed cubic phase directly transforms into  $L_2$  phase at SPC/GDO weight ratio of 25/75.  $Fd3m$  (SPC/GDO weight ratio of 35/65 and 30/70) less stable with increasing temperature

directly converts to  $L_2$  phase, the 2D inverse hexagonal phase (SPC/GDO weight ratios from 65/35 to 50/50) remain persistent, raising the temperature to 42 °C.

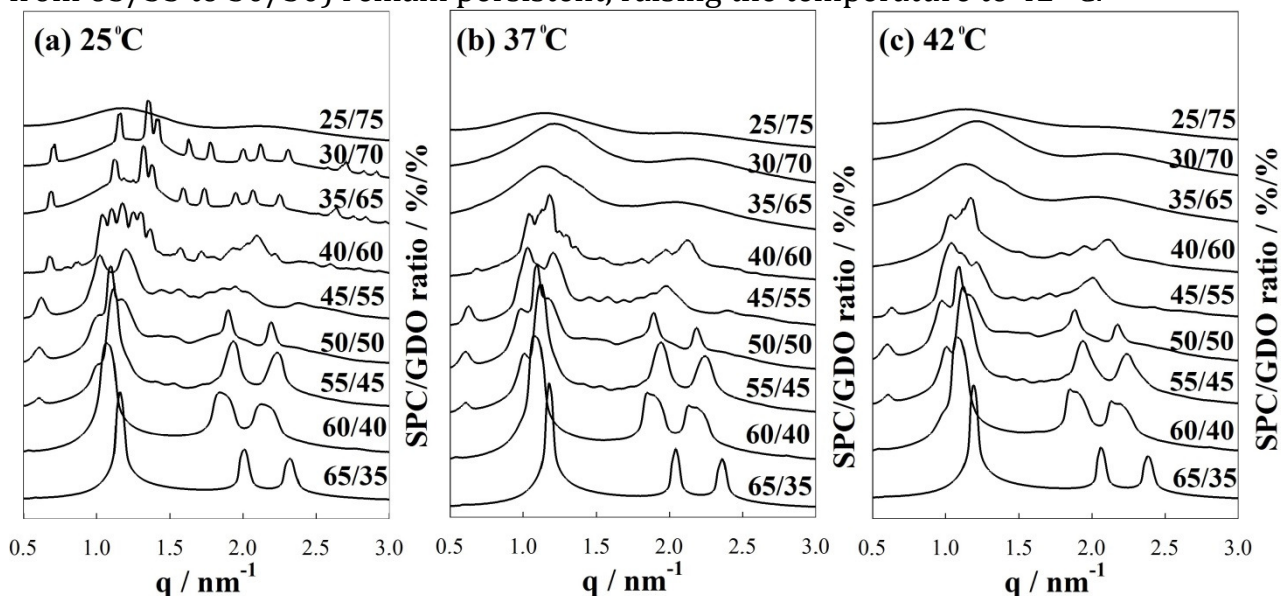


**Figure 5.** SAXD profiles of SPC/GDO mixtures in excess saline

SAXD profiles as a function of lipid composition between SPC/GDO weight ratios of 65/35 and 25/75 at 25 (a), 37 (b), and 42 °C (c).

Instability of inversed cubic phase (space group of  $Fd3m$ ) also observed in fully hydrated SPC/Vitamin E system [22]. In this case, phase changes are less dramatically than in SPC/GDO system. The system is more unstable at physiological temperatures, when GDO content is higher than 62 wt. %. And the phase transition  $I_2 \rightarrow L_2$  is proceeded. 3D hexagonal phase stability decreases with increasing GDO content of the composition. Contrarily, the phase transition  $I_2 \rightarrow L_2$  take place at higher temperatures when GDO content in the mixture decreases. The results obtained allow correlating the release properties with the phase stability at different ambient temperature.

### The phase behavior at the limited hydration

It is still unclear how fast are formed LC phases and how their shell size is associated with the delivery efficiency (Figure 2). The phase behavior of SPC/GDO mixtures weight ratios between 45/55 and 35/65 at the limited hydration (5–40 wt. %) in saline similar to that observed in pure water: i) SPC/GDO weight ratio of 42.5/57.5 in aqueous phase 15–40 wt. % range reverse cubic phase  $Fd3m$  space group formed; ii) SPC/GDO weight ratio of 40/60 in saline 10–30 wt. % range reverse cubic phase  $Fd3m$  space group formed; but in water 10–15 wt. % range cubic phase region is narrower; iv) SPC/GDO weight ratio of 37.5/62.5 in saline 5–40 % range reverse cubic phase  $Fd3m$  space group formed; meanwhile, in water 5–10 % range reverse cubic phase  $Fd3m$  space group and 15–40 % range the "intermediate" phase formed; v) SPC/GDO weight ratio of 35/65 in aqueous phase 15–40 wt. % range reverse cubic phase  $Fd3m$  space group formed. However, the system transitions trends are similar to the full hydration conditions.

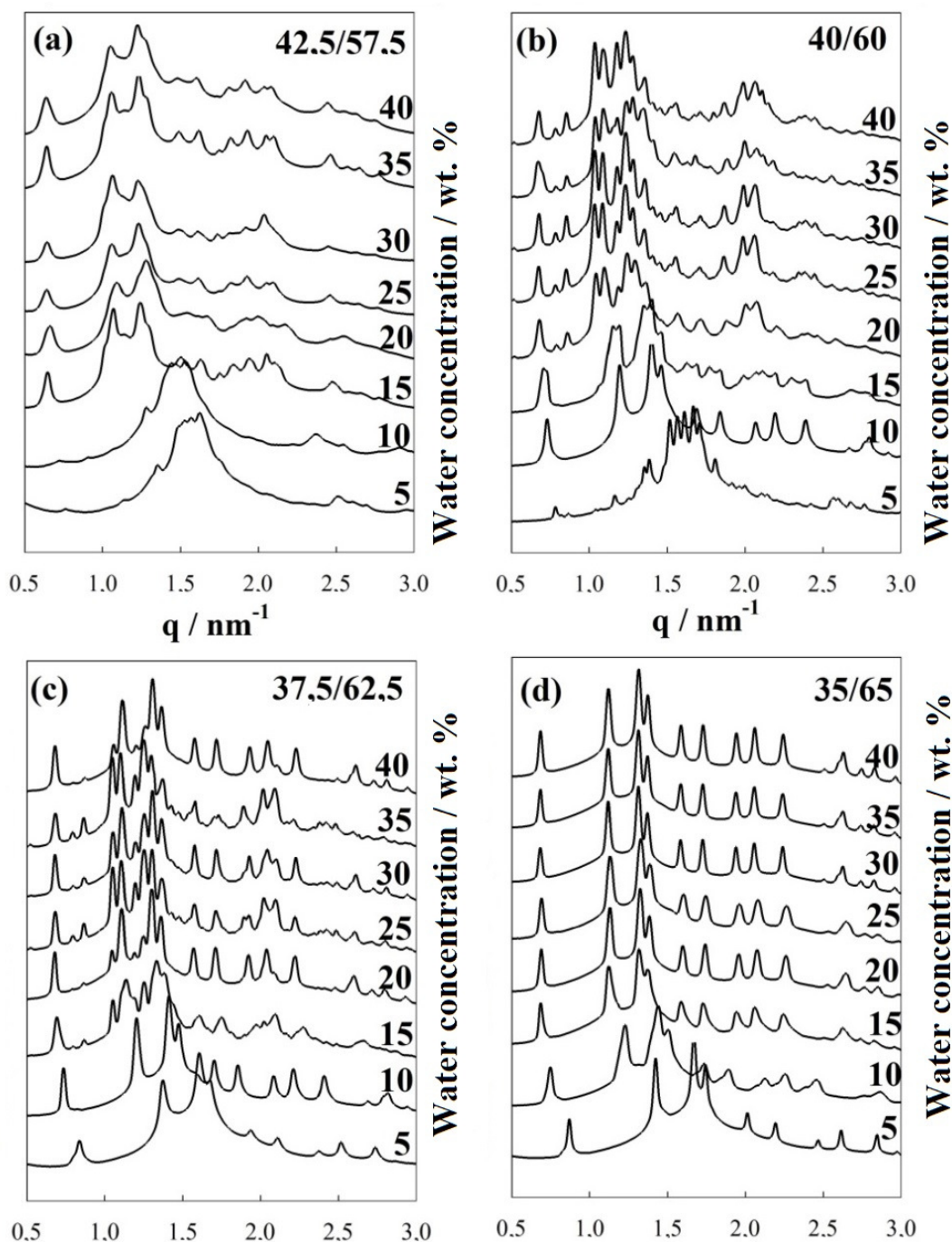


**Figure 6.** SAXD profiles at limited hydration

SAXD profiles at limited hydration (10–40 wt. % of water) of lipid SPC/GDO mixtures weight ratios: a) 42.5/57.5; b) 40/60; c) 37.5/62.5 and d) 35/65, at 25 °C.

### The formation of liquid crystalline shell

LC shell hydration conditions in the capillaries designed to mimic swelling of the subcutaneously injected LC phase pre-formulations. LC shell thickness after 21 days increases with the increase of SPC content in the formulation (Figure 7 a) from 1.5 to 22 mm, SPC/GDO weight ratios 20/80 and 60/40, respectively. **Figure 7 b** presents LC shell formation of two SPC/GDO formulations weight ratios 40/60 and 50/50 in time.

Liquid crystalline phases are formed in first few days after injection. Composition with higher SPC content improves the swelling properties and obviously faster hydration kinetics. Investigations of the swelling behavior of SPC/GDO/saline mixtures provide useful information about swelling kinetics of different lipid soya phosphatidylcholine and glycerol dioleate mixtures.

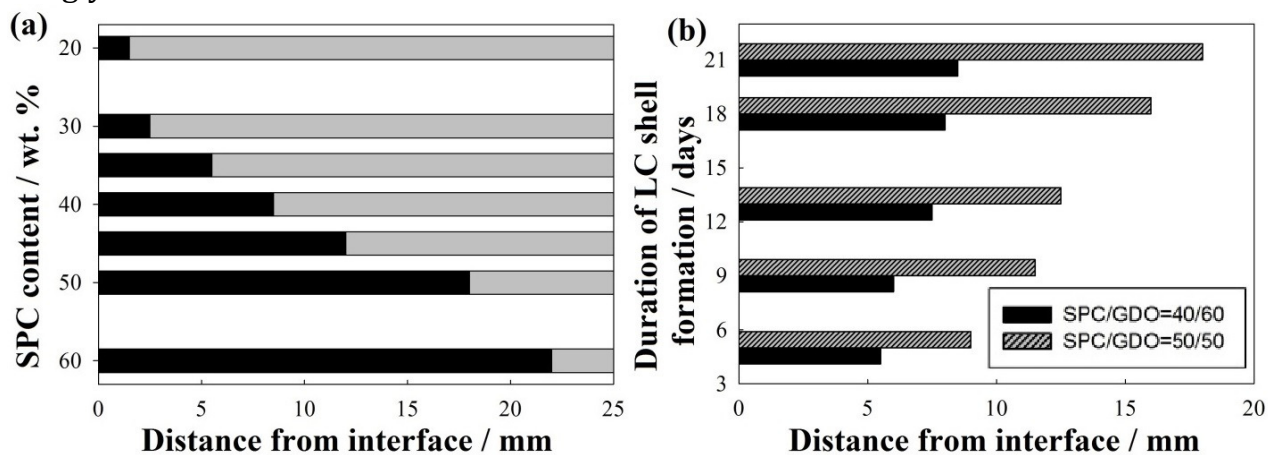


**Figure 7.** The formation of liquid crystalline shell

Liquid crystalline shell formation as a function of SPC content in composition after 21 days (a); Hydration kinetics of LC phase shell formations after: 5, 9, 13, 18 and 21 days (b). Note: dark – SPC/GDO weight ratio 40/60, grey – SPC/GDO weight ratio 50/50. Ethanol was removed in both cases, at 25 °C.

### Function and *in vitro* fluorescein release systems

The main objective was to study the relation between release properties of two-component lipid liquid crystal based drug delivery carriers and the aggregation behavior of particular lipid mixtures. The ultimate goal is to correlate structural/functional carrier properties which would help in designing lipid LC-based long-acting drug release systems. In this part of work we focused on the determination of *in vitro* release properties of SPC/GDO mixtures of various compositions. A cumulative data of Fluo release from various SPC/GDO formulations as a function of composition are presented in **Figure 8**.

An immediate observation from the data in **Figure 8** is that the release of Fluo has a complex behavior depending on SPC/GDO composition. According to the release behavior all formulations may be divided into three groups. The comprising high SPC amounts formulations (SPC/GDO weight ratios 70/30 and 65/35) show massive and fast release of Fluo. Almost all Fluo is released even after few days of incubation. Formulations composed of roughly even amounts of SPC and GDO (between 60/40 and 40/60 by weight) show highly sustained release properties with only several per cents of Fluo being released even after 1 week of incubation. For some of the formulations, especially those between 50/50 and 40/60 of SPC/GDO by weight, the release amount of Fluo was only 2–4 % after one week. Further increase of GDO content in the formulations results in sudden decrease of sustainability. Almost all Fluo is released within a week from the formulations composed of SPC/GDO between weight ratios of 35/65 and 20/80.

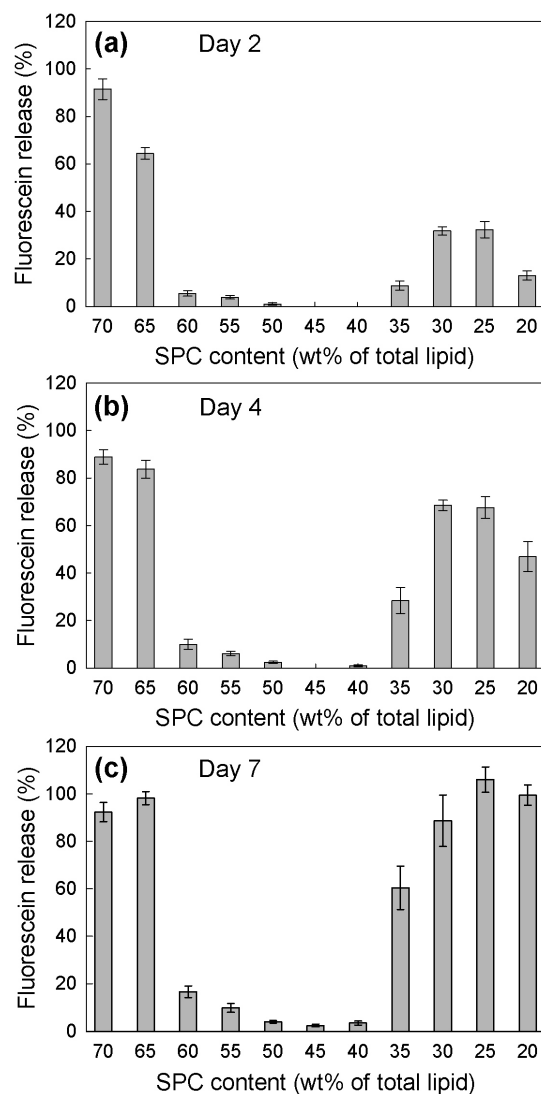


**Figure 8.** Released amount of Fluo from lipid mixture

The released amount of Fluo ( $\pm$ Std. Dev.) after 2 (a), 4 (b) and 7 days (c) as a function of SPC/GDO composition at 37 °C. Triplicate samples for each formulation were used.

In this study used SPC/GDO mixtures comprising 10 wt. % of ethanol distinguish to decrease viscosity. Here the LC phase develops immediately either upon contact with aqueous media present at the site of *in vivo* injection or in contact with buffer solution *in vitro*. In addition, **Figure 9** shows the release kinetics plotted for the formulations possessing sustained release properties as a function of square root of time. The data show that the release of Fluo can be assumed as diffusion controlled with linear dependence vs. square root of time (in all cases  $r^2$  better than 0.98). Such release kinetics behavior is in agreement with previous release studies of other simple lipid LC systems [23]. Note, however, that most of the previous studies of lipid LC as delivery vehicles featured one-component glycerol monooleate (GMO) system which spontaneously forms bicontinuous LC cubic phase when in touch with water [24, 25]. In addition, majority of the studies were performed by using already pre-formed lipid LC phases which, whilst providing somewhat promising release behavior for short

periods of time, are viscous and improbable for actual *in vivo* use. Some improvement of the release properties was achieved by using other synthetic glycerate derivatives showing that the specific LC phase structure is crucial for its sustained release performance [26].

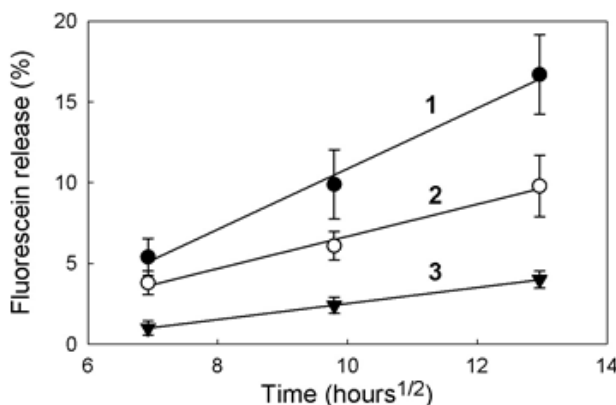


**Figure 9.** Released amount of Fluo as a function of square root of time

Released amount of Fluo ( $\pm$ Std. Dev.) as a function of square root of time for SPC/GDO formulations of 60/40 (1), 55/45 (2) and 50/50 (3) composition by weight at 37 °C. Triplicate samples for each formulation were used.

Also the experiments at two different (25 °C and 37 °C) temperatures were done, to compare the influence of internal structure. For all studied formulations (SPC/GDO weight ratio 60/40; 50/50; 40/60 and 35/65) Fluo release was faster in the higher temperature. It should be noted, that the increase to more relevant temperatures (37–42 °C) influences the stability of  $P6_3/mmc$  (SPC/GDO weight ratio 40/60) and  $Fd3m$  (SPC/GDO weight ratio 35/65) phases (Figure 5). Fluo started to be released from SPC/GDO weight ratio 35/65 only after one week of the incubation at 25 °C. So, the release from reversed micellar phase is rather faster than from discontinuous cubic phase. But the release of fluorescein from  $P6_3/mmc$  (SPC/GDO weight ratio 40/60) phase in both temperatures is characterized as a minimum. Lipid SPC/GDO mixtures which weight ratios between 60/40 and 40/60: the end of  $2D-H2$  phase region  $\rightarrow$  disordered reversed cubic phase of  $Fd3m$  space group  $\rightarrow$  3D hexagonal phase of  $P6_3/mmc$  space group, are most likely for sustained release.

### Summary of the phase behavior of lipid SPC/GDO mixtures

Mixtures of soya phosphatidylcholine and glycerol dioleate form self-assembled structures which were studied with small angle X-ray diffraction. SAXD profiles of these mixtures at 25 °C in aqueous phase excess show variety of reversed nanostructures. It was shown, that by controlling weight ratios of two lipids is possible to create stable drug delivery system with desirable properties. In order to simulate subcutaneous drug injections were performed studies of fluorescein release from lipid SPC/GDO formulations. Also, it have been established that drug release from LC structures is diffusion-dependent.

## II. Lipid liquid crystalline nanoparticles

In this thesis, nanoparticles of dispersed lipid non-lamellar liquid crystalline phases were adsorbed on hydrophilic, hydrophobic and cationic silica surfaces. The influence of surface chemistry, the solution properties and the size of nanoparticles were studied on LCNPs behavior at the interface. In this case, the stability of the nanoparticles is important during the storage, the transport and the target adsorption. Another objective was to study the relation between some of the key properties of the lipid-based drug delivery carriers and the interactions with model and cell membranes. The ultimate goal is to achieve a better understanding of the structural/functional carrier properties and the relation to *in vivo* properties such as toxicity and stability in systemic circulation. The work may also help in designing carrier vehicles for specific administration routes, such as parenteral drug administration. To this end, *in vitro* hemolysis data were complemented with the lipid mixing behavior characteristics of different non-lamellar LCNPs with model phospholipid liposomes, as assessed by FRET measurements (Figure 10).

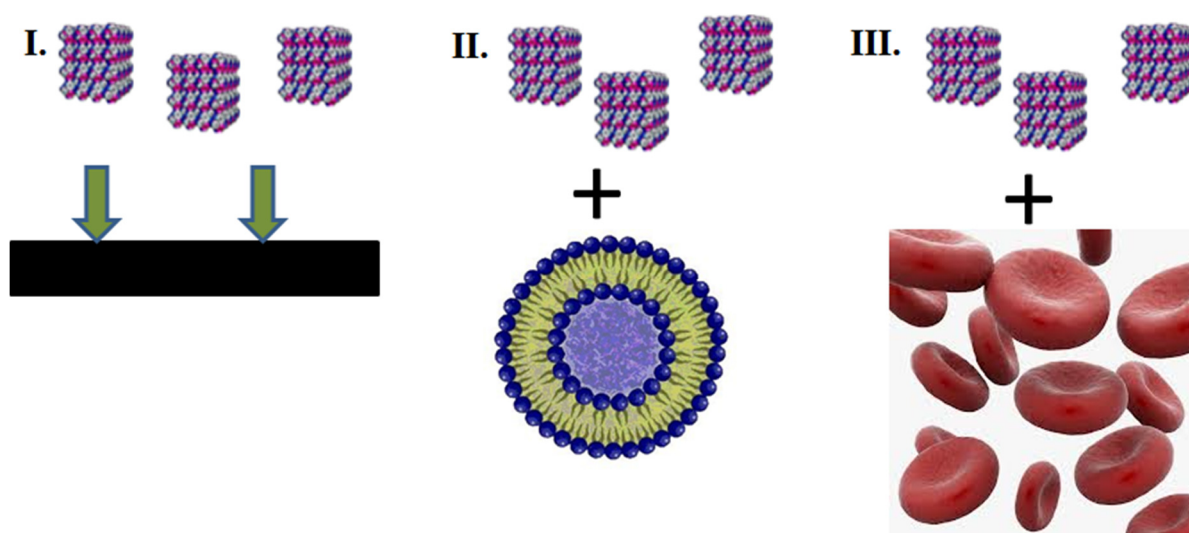


**Figure 10.** Interactions of lipid liquid crystalline nanoparticles

Represented strategies: adsorption (I); fusion with phospholipid liposomes (II) and hemolysis (III).

### Morphology, size and charge control

First of all, the bulk properties of the SPC:GDO/P80 system were studied based on SAXD data in excess solvent conditions at the SPC:GDO ratios of 35:65, 40:60, 50:50, and 60:40 and various contents of P80. Relatively small additions of the surface active ethoxylated monoacyl lipid (P80), used as fragmenting and stabilizing (dispersion) agent in the preparation of the LCNPs, result in rather dramatic phase structure changes. The most dramatic changes are seen for high GDO contents, where for the SPC:GDO weight ratio of 35:65, even 5 wt. % of P80 induces the transformation of the cubic  $Fd3m$  phase into  $L_2$ . Increasing the P80 content to between 10 and 20 wt. % results in the appearance of a  $L_\alpha$  phase. Similar effects of P80 is also observed for SPC:GDO weight ratio of 40:60, where the original 3D hexagonal phase with  $P6_3/mmc$



space group is first transformed into a  $L_2$  phase at about 10 wt. % of P80. With further increase of the amount of stabilizer to above 20 wt. %, the  $L_\alpha$  phase appears.

At equal 50:50 SPC:GDO ratio, several phase transitions are observed with increasing P80 content. At 5 and 10 wt. %, the original  $Fd3m$  phase transforms into an intermediate liquid crystalline phase or phase mixture, characterized by Bragg reflections that we could not unambiguously assign. Because the diffraction pattern for the LCNPs was too weak to be resolved, the corresponding bulk liquid crystalline phases of the same lipid composition were prepared at lower hydration levels. The data show that SPC/GDO without P80 form a reversed micellar cubic phase ( $I_2$ ) in the  $Fd3m$  space group. Therefore, a series of samples with different degrees of hydration with 5–50 wt. % water were investigated. At water contents of  $\leq 15$  wt. %, a reversed hexagonal phase ( $H_2$ ) is formed. At higher levels of hydration, this phase transforms into a lamellar phase ( $L_\alpha$ ). The diffractograms for the  $H_2$  and  $L_\alpha$  phases observed at limited and full hydration, respectively, contain an additional broad diffraction peak that can be attributed to a reversed micellar solution phase ( $L_2$ ). The SAXD data on the swelling behavior and the comparison with the data in the absence of P80 reveal that the SPC:GDO/P80 formulation forms a mixture of  $L_\alpha$  and  $L_2$  phases under full hydration conditions.

Finally, for SPC:GDO weight ratio 60:40, a  $H_2$  phase is formed (a minute fraction of  $Fd3m$  phase is also present at this lipid composition). The additions of 20 wt. % P80 result in a mixture of  $H_2$  and  $L_\alpha$  phases, which on further increase of the P80 content to 40 wt. % is transformed into pure  $L_\alpha$  phase. **Table 2** provides a summary of these results.

**Table 2.** SAXD data summary of SPC:GDO/P80 crystalline structures in excess water (50 wt. %), 25 °C

P80 (%)	SPC/GDO			
	35/65	40/60	50/50	60/40
0	cubic $Fd3m$	3D hexagonal $P6_3/mmc$	cubic $Fd3m$	$H_2+Fd3m$
5	$L_2$	3D hexagonal $P6_3/mmc$	unknown	
10	$L_2+L_\alpha$	$L_2+L_\alpha$	unknown	
20	$L_\alpha$	$L_\alpha$	$L_2+L_\alpha$	$H_2+L_\alpha$
30	$L_\alpha$	$L_\alpha$	$L_\alpha$	
40				$L_\alpha$

Interestingly, the most sensitive phase to P80 additions appears to be the reversed micellar  $Fd3m$  cubic phase, which is the furthest from the normal phases formed by P80 alone in water [27]. It is concluded that P80 promotes the formation of lamellar structures. Interestingly, the transition to lamellar phases occurs at lower P80 content, i.e., reversed cubic micellar phase,  $I_2$ , while the hexagonal phase appears to be structurally more robust, persisting up to at least 20 wt. % P80. Furthermore, the repeat distance  $d$  for the  $L_\alpha$  phase decreases with increasing SPC content. Very similar

effects of P80 on the phase behavior of SPC:GDO are also observed at limited hydration conditions.

Various compositions of SPC:GDO/P80 (35:65/15, 50:50/ 15, 65:35/15, 40:60/20, 50:50/20, and 60:40/20) were prepared, and their size and size distributions were first characterized with dynamic light scattering. These dispersions are quite well-defined, displaying monomodal particle size distributions with diameters ranging between about 240 and 420 nm and with polydispersity indices (PDI) ranging between 0.06 and 0.17, in both cases increasing with the SPC ratio. The surface-to-volume ratio is furthermore dependent on the LCNP size. Thus, in analogy it would be concluded that LCNPs are enriched in GDO in the denser particle core, while the lamellar like shell structures mainly comprise of SPC and, in particular, P80. This also explains the stabilizing ability of P80, resulting from interactions between extending P80 rich lamellar like fragments. In all cases, the shell thickness increases with increasing P80 concentration, where LCNPs stabilized with 20 wt. % of P80 have significantly thicker shell than those with 15 wt. % P80, confirming the notion of the shell enriched with the P80, providing colloidal stability during preparation of the LCNPs and during long-term storage. We note that these are slightly negatively charged, except at the lowest pH studied. The charge is most likely related to the presence of small fractions of fatty acids present in the lipid and P80 samples, which have been observed previously for LCNP systems [28, 29]. The zeta potentials reveal an isoelectric point between pH 3 and 4 and a potential of  $-12$  to  $-17$  mV between pH 5 and 6. Although there is a tendency of a reduction of the negative potential with increasing P80 content, this may be due to more extended lamellar surface domains, and the change is not significant enough to be interpreted quantitatively.

### **The adsorption at the hydrophilic, hydrophobic and cationic silica surfaces**

The effects of particle characteristics and composition on the adsorption of LCNPs were investigated by time-resolved ellipsometry. In this study we have demonstrated that the interfacial interaction between lipid liquid crystalline nanoparticles and surface can be conveniently manipulated by changing the LCNP composition, lipid SPC:GDO ratio, and amount of P80. Increasing the content of P80 stabilizer was found to increase the adsorption of LCNPs at silica.

This study shows how surface chemistry and solvent conditions can be used to control the adsorption of lipid nanoparticles at interfaces. As expected, the largest adsorption was observed on the highly charged cationic surface, where the solution pH greatly affected the adsorption kinetics and also the final adsorbed amount. The adsorption behavior can be classified into three different types depending on the nanoparticles interaction: (1) very strong adsorption and thick layer structures ( $> 8$  mg/m<sup>2</sup> and  $> 60$  nm, respectively) on highly charged cationic surfaces; (2) thick multilayer structures ( $4-6$  mg/m<sup>2</sup> and  $20-35$  nm, respectively) on hydrophilic weakly charged surfaces, and (3) mixed monolayers of lipids ( $< 1$  mg/m<sup>2</sup> and  $1-2$  nm, respectively) on hydrophobic surfaces. The results suggested that the hydrophobic attractive interaction between the lipids and the surface completely disrupts the

nanoparticle structure at hydrophobic surfaces, resulting in the formation of a single monolayer of lipids at the surface that prevents further adsorption. In contrast, LCNPs appear to adsorb relatively intact on highly charged cationic surfaces, resulting in a surface structure composed of individual particles. On hydrophilic weakly charged surfaces such as silica and chitosan-coated silica, intermediate multilayer structures are observed. The mechanism of interaction of LCNPs and the substrate surfaces depends on the substrate chemistry. On the hydrophobic surface, hydrophobic attraction between the substrate surface and the hydrophobic lipid tail results in monolayer coverage. On the cationic surface, electrostatic interaction between the negatively charged LCNPs and the positively charged surface becomes the main driving force for adsorption.

Finally, this study demonstrates that particle formulation can be tailored to control interfacial structure of interest for applications of LCNPs as surface coating and for enhancing drug delivery.

### **The fusion with phospholipid liposomes**

This part of work was focused on determination of the mixing behavior aspects of different LCNPs with soya phosphatidylcholine multilamellar liposomes. **Figure 11** shows the FRET kinetic data obtained from the interaction of GMO/F127, DGMO/GDO/P80, and SPC/GDO/P80 LCNPs with SPC liposomes. As indicated by the fluorescence intensity kinetic decays, GMO-based dispersions showed the highest interaction activity (Figure 11 a). In the presence of SPC liposomes, fluorescence intensities decayed to about 20 % of its initial values within the first 30 min of the mixing experiment. This indicates that the average distance between the fluorescence probes entrapped within the GMO/F127 dispersions rapidly increased, as a result of fast interaction kinetics and lipid mixing of LCNPs with SPC liposomes. As also seen from **Figure 11 a**, there was no lipid mixing behavior dependence on the amount of F127 used to stabilize the GMO-based dispersions.

“Sponge” type LCNP dispersions based on DGMO/GDO/P80 mixtures showed moderate interaction with SPC liposomes (Figure 11 b). In this case, fluorescence intensities decayed to about 85 % of initial values. Note that the fluorescence intensity decays showed a dependence on the amount of P80 used to stabilize the dispersions. DGMO/GDO/P80 dispersions prepared at lipid/P80 weight ratios of 70/30 and 80/20 decayed only about 10 % of the original fluorescence intensity, whereas the dispersions prepared at lipid/P80 weight ratios of 85/15 and 92.5/7.5 decayed 16 and 20 %, respectively. In other words, increased amount of P80 prevented, to some extent, the interaction resulting in lipid mixing of such “sponge” type LCNP dispersions with SPC bilayers. In a recent study was shown that the internal nanostructure of the DGMO/GDO/P80 LCNPs depends on the concentration of P80 [27]. That is, increasing amount of P80 thickens the outer “sponge” phase layer of the nanoparticles in which P80 molecules are preferably located. Therefore, the increasing amount of P80 within the nanoparticles likely provides some additional degree of steric stabilization and restricts fusion/interaction with SPC liposomes. A moderate interaction effect with

SPC liposomes was also observed for hexagonal type LCNPs based on the mixture of DGMO/GDO stabilized with F127 (10 wt. % with respect to lipid mixture). In this case, the fluorescence intensity decayed to about 70 % of its initial value (data not shown).

As seen from the data presented in **Figure 11 c**, aqueous SPC/GDO/P80 dispersions showed a very low degree of interaction with SPC liposomes. Irrespective of SPC/GDO weight ratios (from 70/30 to 10/90) in the dispersion preparations, only a few per cents of the initial fluorescence intensity were lost, indicating practically no lipid mixing with SPC bilayers. To gain insight into interaction features between non-lamellar LCNP dispersions and SPC multilamellar liposomes additional calibration experiments were performed.

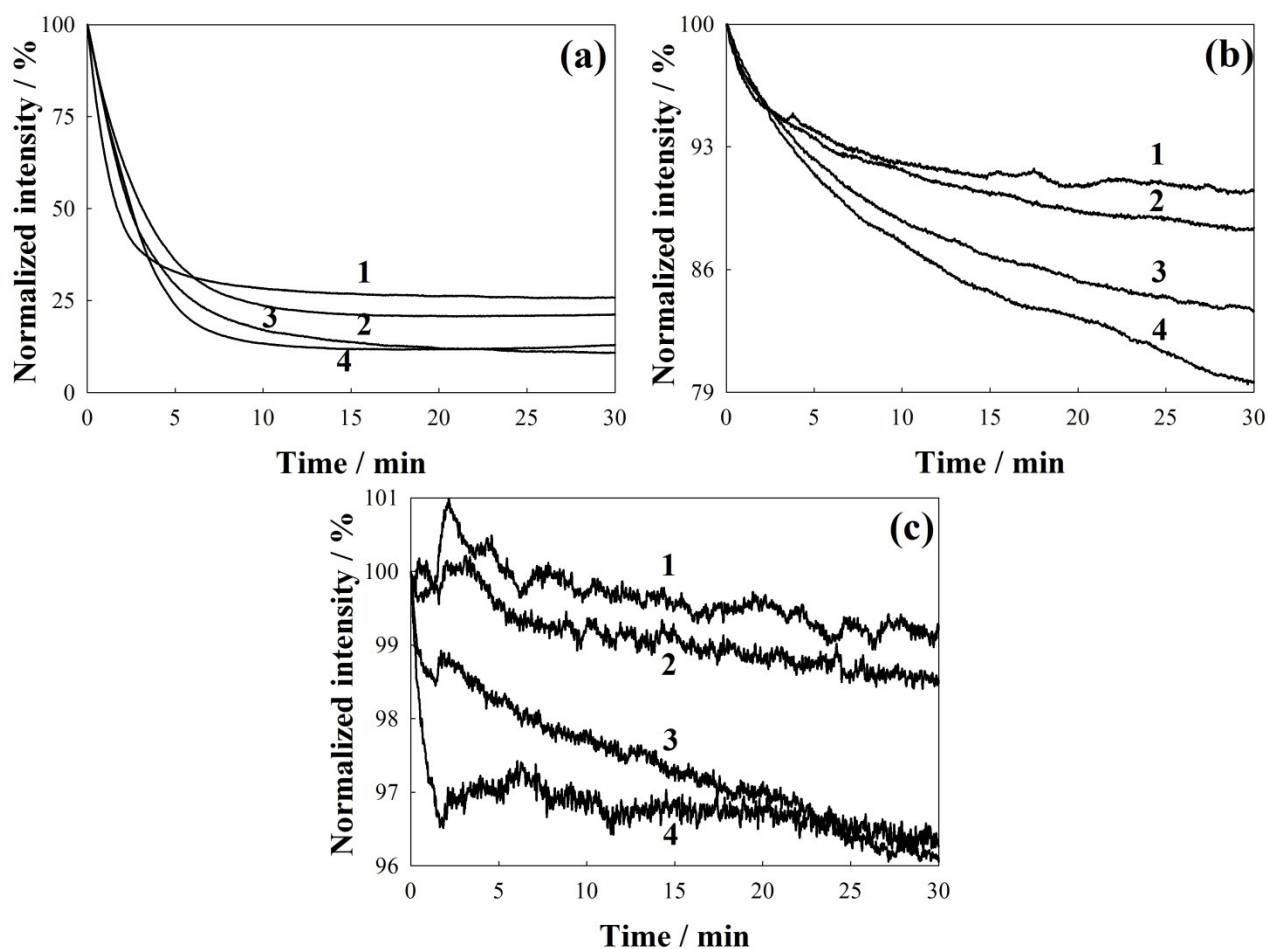


**Figure 11.** FRET fluorescence intensity decays upon mixing of SPC multilamellar liposomes with fluorescently labeled (NBD-PE and DHPE)

(a) GMO/F127 LCNPs at different GMO-to-polymer weight ratios: 70/30 (1), 80/20 (2), 90/10 (3), and 75/25 (4); (b) DGMO/GDO/P80 LCNPs at different lipid (DGMO + GDO)/P80 weight ratios: 80/20 (1), 70/30 (2), 85/15 (3), and 92.5/7.5 (4); and (c) SPC/GDO/P80 LCNPs at different SPC/GDO weight ratios: 70/30 (1), 50/50 (2), 30/70 (3), and 10/90 (4). The excitation wavelength was 463nm and the emission intensity was recorded at 580 nm.

To roughly estimate the lipid bilayer dilution during the mixing process, experiments were performed by measuring the emission intensity at 580 nm at different fluorescent lipid concentrations (total amount of NBD-PE + DHPE) within the

LCNPs. This procedure allows an approximate lipid mixing degree calculation, i.e. to correlate the relative emission decay from the kinetic experiments with the dilution of the fluorescence probes. As expected, the calibration curves showed a near linear decrease in fluorescence intensity with decreasing fluorescence probe concentration. However, especially at low fluorescence probe concentration, the dependencies for the three LCNP dispersions differed slightly. For example, with the SPC/GDO-based LCNP dispersion the fluorescence intensity decreased faster with decreasing probe concentration as compared to the GMO/F127 LCNPs. This observation is most likely related to the different LCNP nanostructural organizations and different localizations and energy transfer features between the fluorescence probes within the respective lipid nanoparticle. Thus, upon mixing of GMO/F127 LCNP dispersions with SPC liposomes, the fluorescence intensities decayed to about 20 % of the initial value (Figure 11 a), indicating a very fast lipid mixing corresponding to more than 10 times dilution of the fluorescence probes within the nanoparticles. Taking into account that experiments were performed at an LCNP/SPC liposome weight ratio of 1/10, it may be concluded that within 30 min, GMO-based LCNPs and SPC liposomes are totally mixed. In contrast, SPC/GDO/P80 LCNPs showed a very limited interaction with SPC liposomes, indicating almost no lipid exchange and practically no dilution of the fluorescence probes. “Sponge” type (DGMO/GDO/P80 based) LCNPs possessed moderate mixing behavior with SPC, corresponding to a limited mass transfer of approximately 1.2 times dilution of the fluorescence probes.

### **The interaction with erythrocytes**

This part of this work was focused on determination of the hemolytic effects of LCNPs of different lipid and polymer compositions on fresh whole blood from rat *in vitro*. Cubic phase dispersions based on GMO/F127 and GMO/P80 at different lipids to polymers (surfactant) weight ratios (90/10, 85/15, 80/20, 75/25, and 70/30) were prepared. As shown in **Table 3**, despite different amounts of stabilizing polymer all GMO/F127 based cubic LCNPs showed massive hemolysis, within the range of 117–137 % relative to positive control. Exchanging the F127 (20 wt. % with respect to GMO) for a different fragmentation agent, P80 (20 wt. %, with respect to GMO), resulted in similar results (136 % hemolysis), indicating no effect of the nature of the fragmentation agent on the hemolytic activity of GMO-based dispersions. The results clearly indicate the limited applicability of the well-known GMO-based dispersions in pharmaceutical products for *i.v.* administration. Hemolytic effects of hexagonal and “sponge” type LCNPs based on mixtures of DGMO/GDO stabilized with F127 (10 wt. %, with respect to lipid mixture) and P80 (7.5, 15, 20, and 30 wt. % with respect to lipid mixture) were also investigated. As seen from the results presented in **Table 3**, despite different structural organizations and natures of the stabilizing/fragmentation agent and its concentration, all DGMO/GDO-based dispersions showed very similar and quite small degree of the hemolytic activity in the order of 1–2 %.

In recent studies have introduced new lipid combinations with applicability for *i.v.* administration, based on mixtures of SPC/GDO/P80 that form stable and

structurally well-defined non-lamellar LCNP dispersions in aqueous media [5, 6]. A number of dispersions stabilized with the same concentration of P80 but at different SPC/GDO weight ratios (70/30, 60/40, 50/50, 40/60, 30/70, 20/80, and 10/90) were prepared and tested (Table 3). The results showed essentially no hemolytic activity relative to positive control for either of the dispersions.

**Table 3.** Results from the hemolysis assay of LCNPs with different lipid compositions mixed with fresh whole blood from rat *in vitro* and particle size data. Hemolysis and particle size data are also provided for the aqueous solution of F127 and P80.

Lipid weight ratio (wt. %)				Fragmentation agent (wt. % with respect to lipid)		Particle size distribution		Hemolysis (%) (n ≥ 3)	
GMO	DGMO/GDO	SPC/GDO	SPC/GDO/GMO	P80	F127	d (nm)	PdI	Mean	SD
100					10	196	0.11	120	14
100					15	199	0.17	114	10
100					20	204	0.17	116	3.4
100					25	206	0.23	114	22
100					30	186	0.26	114	32
100				20		339	0.22	122	16
	50/50				10	154	0.14	1.6	0.2
	50/50			7.5		141	0.14	1.3	0.2
	50/50			15		130	0.16	1.7	0.6
	50/50			20		138	0.21	1.7	0.2
	50/50			30		153	0.23	1.6	0.2
		70/30		20		160	0.17	0.0	0.0
		60/40		20		148	0.18	0.1	0.1
		50/50		20		125	0.20	0.0	0.1
		40/60		20		116	0.20	0.2	0.1
		30/70		20		102	0.24	0.4	0.2
		20/80		20		105	0.22	0.3	0.2
		10/90		20		116	0.20	0.3	0.2
			40/30/30	20		146	0.17	4.2	2.1
			40/24/36	20		141	0.21	4.3	2.1
			40/18/42	20		152	0.13	4.9	2.3
			40/12/48	20		191	0.17	6.2	2.6
			40/6/54	20		236	0.24	11	3.3
			40/0/60	20		226	0.26	18	5.7
				100		11.3	0.11	6.6	1.4
					100	24.4	0.27	0.0	0.0

To complement the above data on the different LCNP formulations, the hemolytic effect of both stabilizing polymer (F127) and surfactant (P80) solutions was also investigated. Micellar solutions of 1 wt. % P80 and 1 wt. % Pluronic F127 were

thus prepared and these resulted in hemolysis of 7 and 0 %, respectively. Thus, P80 per se displays a moderate hemolytic activity when dissolved alone in aqueous solution, as also described elsewhere [30], whereas Pluronic F127 alone appears inert with respect to hemolysis. It is worth noting that 20 wt. % P80 with respect to lipid was used for the SPC/GDO/P80 LCNP dispersions (Table 3) and that the dispersions of 5 wt. % total lipid (mixed 1/1 vol./vol. with rat whole blood) as used in the hemolysis experiments therefore corresponds to a total P80 concentration of 1 wt. %. Thus, when mixed with SPC/GDO, P80 does not induce any measurable hemolysis, i.e. the activity of P80 was significantly reduced in the mixture compared with the pure aqueous P80 solution. A similar effect was observed with DGMO/GDO/P80 LCNP dispersions. Altogether, the results from hemolysis experiments clearly indicate that hemolytic effects of various non-lamellar LCNP dispersions are mostly driven by the nature of lipid molecules and specific lipid composition but not by F127 or P80.

Taken together, there is a relatively good correlation between the determined *in vitro* hemolytic effects of different LCNPs on red blood cells and their mixing behavior with SPC liposomes. As shown in the hemolysis experiments, GMO-based LCNPs display massive hemolysis when mixed with fresh whole blood from rat. Correspondingly, a fast and near complete lipid mixing was observed in FRET experiments with SPC liposomes. SPC/GDO/P80 dispersions, on the other hand, were found to be non-hemolytic and correspondingly the FRET experiments indicated almost no lipid mixing with SPC liposomes.

### **The influence of the glycerol monooleate's concentration**

Interesting results were obtained with the quaternary SPC/GDO/GMO/P80 dispersion system, where GDO was gradually exchanged for GMO to finally obtain a SPC/GMO/P80 mixture (Table 3 and Figure 12 a). The above data (Figure 11 a) clearly showed that GMO can be characterized as highly “fusogenic” with respect to lipid mixing/interaction with SPC liposomes. Indeed, a gradual exchange of GDO for GMO resulted in increased lipid mixing as indicated by the decrease in fluorescence intensity in **Figure 12 a**. When GDO was fully replaced by GMO, the dispersions showed a moderate interaction with SPC liposomes, as fluorescence intensity decayed to about 70% of the initial value. **Figure 12 a** shows the FRET kinetic data obtained from the interaction of quaternary SPC/GDO/GMO/P80 LCNPs with SPC liposomes.

The results showed a gradual increase in hemolytic activity from 0.2 % (GDO/GMO; 100/0 wt. %/wt. %) to 18 % when GDO within the LCNP dispersions, was fully replaced by GMO (GDO/GMO; 0/100 wt. %/wt. %). The observed behavior of the SPC/GDO/P80 LCNP dispersions in the presence of the highly hemolytic active GMO shows that SPC/GDO/P80 based dispersions can accommodate considerable amounts of monoglyceride (or GMO) “impurities” and still possess low hemolytic activity.

It is interesting to note the dramatic effect of GMO on both lipid mixing and hemolysis. The critical aggregation concentration (*cac*) or critical micelle concentration (*cmc*) of GMO has been determined to be approximately  $4 \times 10^{-6}$  M [31] and GMO has a much higher monomer activity compared with SPC and GDO that have

estimated *cacs* (or *cmcs*) in the  $10^{-9}$  to  $10^{-10}$  M range [32]. When GMO is mixed with SPC/GDO, hemolysis and lipid mixing decrease markedly compared with the pure GMO system, but increase gradually with the fraction of GMO in the lipid mixture (Figure 12). These effects can be explained by lowering the GMO monomer activity in the mixture. Assuming ideal mixing, one can roughly calculate the *cac* (*cmc*) for the lipid mixture, e.g. for the mixtures displayed in **Table 3**. Taking as an example the SPC/GMO/P80 32/48/20 mixture, with *cac* (or *cmc*) values of  $10^{-9}$  M,  $4 \times 10^{-6}$  M and  $6 \times 10^{-6}$  M [33], for SPC, GMO and P80, respectively, and using Eq. (4) (where  $\alpha_i$  is *cmc<sub>i</sub>* the *i*th component mole fraction and *cmc*, respectively), the mixed *cmc* is estimated to approximately  $5 \times 10^{-9}$  M.

$$\frac{1}{cmc_{mixed}} = \sum_i \left( \frac{\alpha_i}{cmc_i} \right) \quad (4)$$

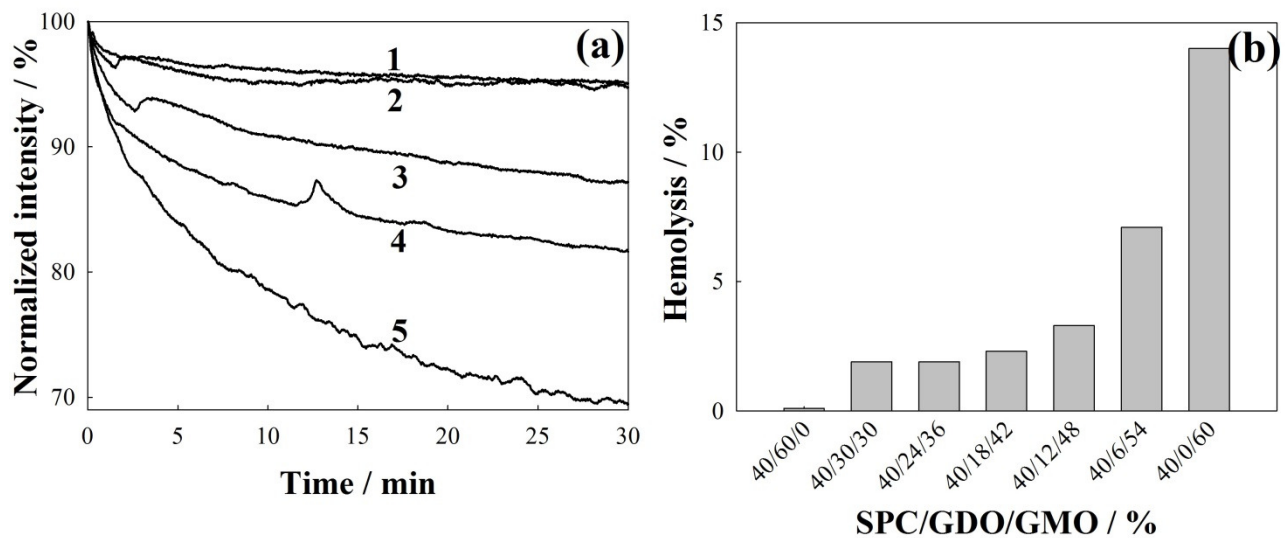


**Figure 12.** The influence of the glycerol monooleate's concentration

FRET fluorescence intensity decays upon mixing of SPC multilamellar liposomes with fluorescently labeled (NBD-PE and DHPE) SPC/GDO/GMO/P80 LCNPs at different SPC/GDO/GMO weight ratios: 40/45/15 (1), 40/60/0 (2), 40/30/30 (3), 40/18/42 (4) and 40/0/60 (5). The excitation wavelength was 463nm and the emission intensity was recorded at 580 nm (a). Hemolysis of rat whole blood induced by lipid LCNP dispersions based on SPC/GDO/GMO/P80 at different SPC/GDO/GMO ratios (40/60/0, 40/30/30, 40/24/36, 40/18/42, 40/12/48, 40/6/56 and 40/0/60). The P80 concentration was in all cases 20 wt. % with respect to the other lipid components (see also Table 3). Note the practical absence of hemolysis for the SPC/GDO/P80 dispersion (b).

Clearly, the cubic phase forming GMO has more pronounced membrane destabilizing effects and this may be related to potential phase segregation within the cell membrane introducing pore structures and resulting in leakage of the cellular content. This type of pore formation may also occur in normal surfactant/lipid membrane system [34], but depending on the molecular nature of the surfactant, is generally not causing highly leaky lipid membranes until a relatively high fraction of the surfactant is present in the lipid bilayer. Hence, in addition to chemical activity, the local effect of a lipid or surfactant drug delivery vehicle constituent on cell membrane



structural properties appears to play a role for its hemolytic activity and its ultimate qualification as drug delivery agent.

### **Summary of interactions of lipid liquid crystalline nanoparticles**

It was shown that the interaction between LCNPs and the surface at the interface can be adequately controlled by simply changing the LCNPs composition, i.e. lipid SPC/GDO ratio and the content of Polysorbate 80. The results suggested that the hydrophobic attractive interaction between the lipids and the surface completely disrupts the LCNP structure at hydrophobic surfaces, resulting in the formation of a single monolayer of lipids at the surface that prevents further adsorption. In contrast, LCNPs appear to adsorb relatively intact on highly charged cationic surfaces, resulting in a surface structure composed of individual particles. On hydrophilic weakly charged surfaces intermediate multilayer structures are observed. Also, LCNPs based on lipid SPC/GDO mixtures limited mixing with phospholipid liposomes and has no hemolytic activity. Both independent tests correlate with each other.

### **CONCLUSIONS**

1. Soya phosphatidylcholine (SPC) and glycerol dioleate (GDO) based mixtures in excess water with increasing GDO content at 25 °C undergo these phase transitions: lamellar → reverse 2D hexagonal → reversed micellar *Fd3m* cubic → reversed micellar *P6<sub>3</sub>/mmc* hexagonal → undetermined structures → *Fd3m* → reversed micellar solution.
2. The transition of liquid crystalline phases of lipid SPC/GDO-based mixtures into disordered structure with increasing GDO content proceeds at lower temperatures.
3. A minimum of fluorescein release from lipid SPC/GDO-based liquid crystal monolith at 37 °C is observed when a mixture of a reversed micellar *Fd3m* cubic and *P6<sub>3</sub>/mmc* hexagonal phases is formed.
4. The nanoparticles dispersion of lipid SPC/GDO liquid crystalline phases by adsorbing on hydrophobic and hydrophilic silica surfaces form a monolayer and multilayer, respectively. Meanwhile, nanoparticles on cationic silica surface adsorb intact.
5. Dispersions of nanoparticles based on mono- and diglycerides are characterized by strong fusion with phospholipid liposomes and hemolytic activity. Nanoparticles of dispersed lipid SPC/GDO liquid crystalline phases in comparison with these dispersions aren't characterized by such properties.
6. It was found that the fusion of nanoparticles of dispersed lipid SPC/GDO and glycerol monooleate mixtures and their hemolytic effect do not change when the concentration of glycerol monooleate in the mixtures is less than 30 %.

## ACKNOWLEDGEMENTS

This is one of the most exciting pages for me in this thesis. I am deeply thankful to all who contributed to the preparation of this work. During these four wonderful years I've met lots of people who supported and motivated my study and my PhD work. Without my supervisor, colleagues, family and friends I'd not handle that alone.

First of all, this thesis would not have been possible without my supervisor dr. **Justas Barauskas**. He led me into the exciting world of science, and carefully guided me to become a researcher. I appreciated his knowledge ability, seriousness, patience, and especially his constant effort in critically reading my writings.

Collaboration in research is an excellent experience. I am gratified to have the chance to work with the foremost authorities **Vitaly Kocherbitov** (Malmö University, Sweden) and **Daniel Topgaard** (Lund University, Sweden). Also, for financial support and scientific collaboration I would like to thank the project partners from pharmaceutical company Camurus AB (Sweden): **Markus Johnsson** and **Fredrik Tiberg**; and, also, the co-authors of papers: **Camilla Cervin**, **Debby P. Chang** and **Tommy Nylander**; for technical support in SAXD experiments at the MAX-lab (Lund, Sweden): **Yngve Cerenius**, **Tomás Plivelic** and **Dörthe Haase**. My joyful life in Sweden would have been incomplete without: **Yana**, **Vida**, **Sanna**, **Nina** and **Marianna**. I have to thank my colleagues from Vilnius University Institute of Biochemistry, in particular **Edita**, **Rima**, **Tadas**, **Marius**, **Mindaugas** for great contributing to the daily relaxing coffee breaks.

Special thanks go to the *Lithuanian State Studies Foundation*; the *Camurus Lipid Research Foundation*; *Swedish Institute VISBY programme* and *The Research Council of Lithuania* for funding my PhD study. And thanks for Department of Bioelectrochemistry and Biospectroscopy (Vilnius University Institute of Biochemistry) for given lab space.

Last, but not the least, thanks to my mom and dad being patient with me. And thanks to my friends **Ieva**, **Remigijus** and **Indrė** for nice and cosy Jazz Mondays.

## REFERENCES

1. Luzzati V. In: Chapman D. (ed.), *Biological membranes*. Vol. 1, Academic Press: New York, 1968: 71–123.
2. Shah J., Sadhale Y., Chilukuri D. M. *Adv. Drug Del. Rev.* 2001 (47): 229–250.
3. Bergenståhl B. A., Stenius P. *J. Phys. Chem.* 1987 (91): 5944–5948.
4. Borné J., Nylander T., Khan A. *Langmuir* 2000 (16): 10044–10054.
5. Johnsson M., Barauskas J., Norlin A., Tiberg F. *J. Nanosci. Nanotechnol.* 2006 (6): 3017–3024.
6. Cervin C., Vandoolaeghe P., Nistor C., Tiberg F., Johnsson M. *Eur. J. Pharm. Sci.* 2009 (36): 377–385.
7. Vandoolaeghe P., Barauskas J., Johnsson M., Tibeg F., Nylander T. *Langmuir* 2009 (25): 3999–4008.
8. Vandoolaeghe P., Rennie A. R., Campbell R. A., Thomas R. K., Hook F., Fragneto G., Tiberg F., Nylander T. *Soft Matter* 2008 (4): 2267–2277.
9. Orädd G., Lindblom G., Fontell K., Ljusberg-Wahren H. *Biophys. J.* 1995 (68): 1856–1863.
10. Cerenius Y., Stahl K., Svensson L. A., Ursby T., Oskarsson A., Albertsson J., Liljas A. *J. Synchrotron Rad.* 2000 (7): 203–208.
11. Knaapila M., Svensson C., Barauskas J., Zackrisson M., Nielsen S. S., Toft K. N., Vestergaard B., Arleth L., Cerenius Y. *J. Synchrotron Rad.* 2009 (16): 498–504.
12. provided by Dr. A. Hammersley (<http://www.esrf.fr/computing/scientific/FIT2D>)
13. Struck D. K., Hoekstra D., Pagano R. E. *Biochemistry* 1981 (20): 4093–4099.
14. Tiberg F., Landgren M. *Langmuir* 1993 (9): 927–932.
15. Vandoolaeghe P., Tiberg F., Nylander T. *Langmuir* 2006 (22): 9169–9174.
16. De Feijter J. A., Benjamins J., Veer F. A. *Biopolymers* 1978 (17): 1759–1772.
17. Rosenbaum E., Tavelin S., Johansson L. B.-Å. *Int. J. Pharm.* 2010 (388): 52–57.
18. Shearman G. C., Tyler A. I. I., Brooks N. J., Templar R. H., Ces O., Law R. V., Seddon J. M. *J. Am. Chem. Soc.* 2009 (131): 1678–1679.
19. Zeng X., Liu Y., Imperor-Clerc M. *J. Phys. Chem. B* 2007 (111): 5174–5179.
20. Seddon J. M. *Biochemistry* 1990 (29): 7997–8002.
21. Luzzati V., Vargas R., Gulik A., Mariani P., Seddon J. M., Rivas E. *Biochemistry* 1992 (31): 279–285.
22. Barauskas J., Cervin C., Tiberg F., Johnsson M. *PCCP* 2008 (10): 6483–6485.
23. Phan S., Fong W., Kirby N., Hanley T., Boyd B. *Int. J. Pharm.* 2011 (421): 176–182.
24. Drummond C. J., Fong C. *Curr. Opin. Colloid Interface Sci.* 1999 (4): 449–456.
25. Peng X. S., Wen X. G., Pan X., Wang R. C., Chen B., Wu C. B. *AAPS PharmSciTech* 2010 (11): 1405–1410.
26. Boyd B. J., Whittaker D. V., Khoo S.-M., Davey G. *Int. J. Pharm.* 2006 (309): 218–226.
27. Barauskas J., Misiunas A., Gunnarsson T., Tiberg F., Johnsson M. *Langmuir* 2006 (22): 6328–6334.
28. Shen H. H., Crowston J. G., Huber F., Saubern S., McLean K. M., Hartley P. G. *Biomaterials* 2010 (31): 9473–9481.
29. Svensson O., Thuresson K., Arnebrant T. *Langmuir* 2008 (24): 2573–2579.
30. Miwa A., Ishibe A., Nakano M., Yamashira T., Itai S., Jinno S., Kawahara H. *Pharm. Res.* 1998 (15): 1844–1850.
31. Ho S. -Y., Storch J. *Am. J. Physiol. Cell Physiol.* 2001 (281): 1106–1117.
32. Tanford C. 2nd ed. Krieger Publishing Company, Florida, 1991.
33. Thorsteinsson M. V., Richter J., Lee A. L., DePhilips P. *Anal. Biochem.* 2005 (340): 220–225.
34. Edwards K., Almgren M. *Langmuir* 1992 (8): 824–832.

# LIPIDŲ SKYSTAKRISTALINIŲ VAISTŲ NEŠIKLIŲ SAVYBIŲ IR JŲ SĄVEIKŲ SU LAŠTELIŲ MEMBRANŲ MODELIAIS TYRIMAS

## REZIUMĖ

Darbo tikslas – lipidų skystakristalių vaistų nešiklių, suformuluotų sojos fosfatidilcholino (SPC), glicerolio dioleato (GDO) ir vandens pagrindu, struktūrinių savybių ir sąveikų su skirtingais paviršiais tyrimas. Darbe tirtos lipidų SPC/GDO mišinių skystųjų kristalų (SK) fazės ir disperguotų fazių nanodalelės (LSKN). Sumodeliuotos atitinkamos dalinės ir visiškos hidratacijos sąlygos. Pateikta sąsaja tarp SK struktūros ir aktyvių medžiagų išėjimo iš jų funkcijos. Sukurtos atitinkamų sąveikų su skirtingais paviršiais modelinės sąlygos.

Nustatyta, jog, keičiant SPC ir GDO tarpusavio santykį, kontroliuojamas ir keičiamas įterptos medžiagos uždelstas išėjimas. Lipidų SPC/GDO mišinių skystakristalės nanodalelės pasižymi žemu hemoliziniu aktyvumu ir labiau nei kiti tirti lipidų mišiniai tinka intraveniniam vaistų pernešimui. Pirmąkart iširtos šių LSKN adsorbcinės savybės ant skirtingų silicio paviršių. Keičiant paviršiaus savybes, galima kontroliuoti disperguotų lipidų SPC/GDO skystakristalių fazių nanodalelių adsorbciją. LSKN tyrimai *in vitro* leidžia prognozuoti jų elgesį *in vivo*.

Šie tyrimų rezultatai leis spręsti apie tolimesnį analizuotų lipidų mišinių panaudojimą, kuriant aktyvių biologinių medžiagų nešiklius. Taps lengviau programuoti ir sukonstruoti norimų savybių vaistų nešiklį.

### Darbo išvados:

1. Sojos fosfatidilcholino (SPC) ir glicerolio dioleato (GDO) mišiniai vandens pertekliuje, didėjant GDO daliai ir 25 °C temperatūroje, patiria tokius fazinius virsmus: lamelinė → atvirkštinė 2D heksagoninė → atvirkštinių micelių *Fd3m* kubinė → atvirkštinių micelių *P6<sub>3</sub>/mmc* heksagoninė → nenustatytos struktūros → *Fd3m* → atvirkštinių micelių tirpalas.
2. Lipidų SPC/GDO mišinių atvirkštinių skystakristalių fazių perėjimas į netvarkingą struktūrą vyksta, didėjant GDO daliai, žemesnėse temperatūrose.
3. Fluoresceino išėjimo iš lipidų SPC/GDO mišinių skystojo kristalo monolito minimumas 37 °C temperatūroje stebimas, kai formuojamas atvirkštinių micelių *Fd3m* kubinės ir *P6<sub>3</sub>/mmc* heksagoninės fazių mišinys.
4. Adsorbavusios disperguotų lipidų SPC/GDO mišinių skystakristalės nanodalelės ant hidrofobinio ir hidrofilinio silicio paviršių atitinkamai formuoja monosluoksnį ir daugiasluoksnį. O ant katijoninio silicio paviršiaus nanodalelės adsorbuojasi nepažeistos.
5. Disperguotų monogliceridų ir digliceridų mišinių nanodalelės pasižymi stipriu susiliejimu su fosfolipidų liposomomis ir hemoliziniu poveikiu. O, lyginant su šiomis dispersijomis, disperguotų lipidų SPC/GDO mišinių nanodalelės nepasižymi šiomis savybėmis.
6. Nustatyta, jog disperguotų lipidų SPC/GDO ir glicerolio monooleato mišinių nanodalelių susiliejimo stipris su fosfolipidų liposomomis ir hemolizinis poveikis nekinta, kai glicerolio monooleato koncentracija mišinyje mažesnė nei 30 %.

## CURRICULUM VITAE

---

JANKUNEC MARIJA  
1983-12-05, Vilnius

### Contact address:

VU Institute of Biochemistry, Mokslininkų 12, Vilnius  
E-mail: marija.jankunec@bchi.vu.lt

### Education

1990-2002                      Graduation certificate of Vilnius J. Lelevel Secondary school.  
2002-2006                      Vilnius Gediminas Technical University, bachelor degree in  
bioengineering.  
2006-2008                      Vilnius University, master degree in biochemistry.  
2008 - 2012                      Doctoral studies at Institute of Biochemistry, Vilnius University.

### Work/practice experience

2004 july                      Training internship, Institute of Biotechnology, Vilnius.  
2005 july                      Industrial internship, Customs Laboratory, Vilnius.  
2006                              Bachelor degree final thesis: *Observation of Saccharomyces cerevisiae with the atomic force microscope*, supervisor: prof. habil. dr. V. Snitka (KTU RC Microsystems and Nanotechnology).  
2007 - 2008                      Master degree final thesis: *Investigations of interactions of lipid liquid crystalline nanoparticles with model and biomimicking surfaces with atomic force microscopy*, supervisor: dr. J. Barauskas (VU Institute of Biochemistry).  
2008 06-2009 05                Technician, CJC COWI Baltic.  
2008 10-2010 12                Laboratory assistant, Institute of Biochemistry.  
2012 10-till now                Specialist, VU Institute of Biochemistry.

### Internship in the foreign research centers

2008-2011                      Six visits, for 2-6 days long, in the Synchrotron radiation research center MAX-Lab (Lund University, Sweden).  
2010-2011                      Four visits, total duration of all visits 7.5 months, in the Department of Biomedical Science, Faculty of Health and Society, Malmö University (Sweden).  
2011 01-03                      Kemicentrum, the Division of Physical and Theoretical Chemistry, Lund University (Sweden).

### Awards

2010-2012                      "Promotional scholarships for doctoral candidates", Lithuanian State Studies Foundation and The Research Council of Lithuania.  
2011                              "Support for PhD students' internships" grant, The Research Council of Lithuania.  
2012 spring                      "Support for students' scientific research" supervisor's grant, The Research Council of Lithuania.  
2012 summer                      "Students' research practice" supervisor's grant, The Research Council of Lithuania.  
2012                              "Funding of research visits" grant, The Research Council of Lithuania.